Title
Role of Interleukin-22 in Tumor Angiogenesis

Author
Protopsaltis, Nicholas James

Publication Date
2017

Peer reviewed|Thesis/dissertation

UNIVERSITY OF CALIFORNIA, SAN DIEGO

Role of Interleukin-22 in Tumor Angiogenesis

A dissertation submitted in partial satisfaction of the requirements for the degree
Doctor of Philosophy

in

Biomedical Sciences

by

Nicholas James Protopsaltis

Committee in charge:

Professor Napoleone Ferrara, Chair
Professor Steven Gonias, Co-Chair
Professor Nigel Calcutt
Professor Daniel Donoghue
Professor Dwayne Stupack

2017

This Dissertation of Nicholas James Protopsaltis is approved, and it is acceptable in quality and form for publication on microfilm and electronically:

Co-Chair

Chair

University of California, San Diego

2017

TABLE OF CONTENTS

LIST OF ABBREVIATIONS

AHR	Aryl hydrocarbon receptor
AKT	Ak strain transforming (Protein kinase B)
ANOVA	Analysis of variance
Bcl-X_L	B-cell lymphoma-extra large
bFGF	Basic fibroblast growth factor
Cas9	CRISPR associated protein 9
CRISPR	Clustered regularly interspaced short palindromic repeats
CXC	α-chemokine
DMEM	Dulbecco's modified Eagle medium
EGFR	Epidermal growth factor receptor
EBM-2	Endothelial basal medium (2)
EGM-2	Endothelial growth medium (2)
ELISA	Enzyme-linked immunosorbent assay
ERK	Extracellular signal–regulated kinases
FACS	Fluorescence-activated cell sorting
FBS	Fetal bovine serum
G-CSF	Granulocyte-colony stimulating factor
HUVEC	Human umbilical vein endothelial cell
IgG	Immunoglobulin G
IL	Interleukin
JAK	Janus tyrosine kinase

KO	Knockout
Maf	musculoaponeurotic fibrosarcoma
MVEC	Microvascular endothelial cell
NF-kB	nuclear factor kappa-light-chain-enhancer of activated B cells
NP1/NP2	Neuropilin 1 / Neuropilin 2
PBS	Phosphate buffered saline
PTEN	Phosphatase and tensin homolog
RAG	Recombination activating gene
RIPA	Radioimmunoprecipitation assay buffer
RORC	retinoic acid receptor related orphan receptor C
RTK	Receptor tyrosine kinase
SDS-PAGE	Sodium dodecyl sulfate polyacrylamide gel electrophoresis
SH2	Src Homology 2
siRNA	Small interfering ribonucleic acid
Src	sarcoma (kinase)
STAT	signal transducer and activator of transcription
TGF-β	Transforming growth factor Beta
TYK	Tyrosine kinase
VEGF	Vascular endothelial growth factor
WT	Wild type

LIST OF FIGURES

ACKNOWLEDGEMENTS

I would like to thank my advisor Dr. Napoleone Ferrara for providing me with the resources and guidance to pursue my research. I appreciate all of the Ferrara lab members for helping to create a supportive environment, and in particular to Wei Liang and Qin Li for so graciously lending their assistance.

I would also like to thank the MSTP for giving me the opportunity to pursue my medical and scientific education at UCSD. Dr. Paul Insel and Dr. Neil Chi have been incredibly supportive of me, which I appreciate tremendously. Finally, I would like to acknowledge the invaluable help of Mary Alice Kiisel over my years at UCSD.

Chapter 2, in part, is currently being prepared for submission for publication of the material. Protopsaltis, N.; Liang, W.; Nudleman, E.; Ferrara, N. The dissertation author was the primary investigator and author of this material.

Chapter 3, in part, is currently being prepared for submission for publication of the material. Protopsaltis, N.; Liang, W.; Nudleman, E.; Ferrara, N. The dissertation author was the primary investigator and author of this material.

Chapter 4, in part, is currently being prepared for submission for publication of the material. Protopsaltis, N.; Liang, W.; Nudleman, E.; Ferrara, N. The dissertation author was the primary investigator and author of this material.

VITA

2011 Bachelor of Science, Biochemistry, Summa Cum Laude
Saint Louis University

2011-2013 Medical Student, Medical Scientist Training Program
University of California – San Diego, School of Medicine

2013-2017 Graduate Student, Biomedical Sciences
University of California – San Diego, School of Medicine

2017 Doctor of Philosophy, Biomedical Sciences
University of California – San Diego, School of Medicine

2018-2020 Medical Student, Medical Scientist Training Program
University of California – San Diego, School of Medicine

ABSTRACT OF THE DISSERTATION

Role of Interleukin-22 in Tumor Angiogenesis

by

Nicholas James Protopsaltis

Doctor of Philosophy in Biomedical Sciences

University of California, San Diego, 2017

Professor Napoleone Ferrara, Chair

There is increasing recognition that the immune system plays a crucial role in either the promotion or inhibition of tumor development and growth. Current models of tumorigenesis rely on cells' ability to evade the immune system. Escaping immune-mediated destruction, however, is only one step in the beginning of tumor growth. While many types of immune cells have been

implicated in cancer progression or suppression, the T_H17 subset of CD4+ helper T cells is of particular interest due to their clinical implication as being a negative prognostic indicator in some types of cancer, and a positive indicator in others. T_H17 cells produce two main cytokines: their hallmark cytokine interleukin-17, and interleukin-22. Interleukin-22 is known for exhibiting a multitude of effects in different types of epithelium, but its role in angiogenesis is only beginning to be elucidated.

This study begins by examining the effects of interleukin-22 on endothelial cells *in-vitro*. It was found that IL-22 stimulates endothelial cell proliferation, survival, and chemotaxis. It also induces activation of the STAT3, MAPK, and AKT pathways in endothelial cells, consistent with its known signaling effects in cells of epithelial origin.

The mouse T cell lymphoma EL4 was used as a tumor model for a number of *in-vivo* studies. It was found that these tumors produce interleukin-22 both *in-vitro* and *in-vivo*, and that blockade of IL-22 *in-vivo* results in a statistically significant decrease in tumor growth in C57BL/6, athymic nude, and Rag $1^{-/-}$ mice. Additionally, it was observed that anti-IL22 antibody therapy decreased blood vessel density within EL4 tumors.

A mouse glioblastoma cell line, GL261, was also investigated to determine the role of interleukin-22 in tumor growth and angiogenesis. IL-22 blockade resulted in decreased tumor growth in both C57BL/6 and athymic nude tumor bearing mice.

In summation, the data observed indicates that interleukin-22 can directly act on endothelial cells to induce angiogenesis. Furthemore, blocking IL-22 *in-vivo* results in a statistically significant reduction in tumor growth using multiple tumor models.

CHAPTER 1.

Introduction to Angiogenesis, Immune Cells in the Tumor Microenvironment, and Interleukin-22

1.1 - Angiogenesis is the formation of new blood vessels.

The term originated in 1935 to describe the formation of blood vessels in the placenta, and it has subsequently been shown to play a role in both normal and pathologic states[1]. In the 1960's, it was demonstrated that solid tumors depend on this process for their own growth, and that a diffusible factor could induce tumor neovascularization[2]. While these earlier experiments showed that a "humoral factor" could pass through a membrane and recruit blood vessels, Judah Folkman eventually identified a product secreted from tumor cells, which he called TAF or "tumor-angiogenesis factor," that was mitogenic on endothelial cells and could induce the formation of new capillaries[3]. Furthermore, it was shown that initially slow growing tumors rapidly increased in size after receiving a vascular supply (Figure 1) [4]. Additional work revealed that TAF could induce neovascularization in multiple settings, and importantly, that there may be a unique receptor for TAF on endothelial cells which could be blocked as a way of inhibiting tumor aniogenesis[5].

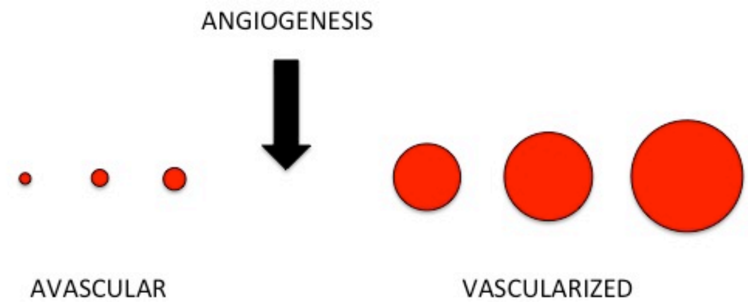

Figure 1: Angiogenesis is a Rate Limiting Step For Tumor Growth. Adapted from Folkman, J 1975.

In 1983, a factor was identified that induced vascular leakage, and was termed vascular permeability factor, or VPF[6]. VPF was not purified to homogeneity or sequenced at the time, and although the researchers did not know of its mitogenic activity, this same factor was later determined to be vascular endothelial growth factor, or VEGF[7]. VEGF was identified, isolated, purified, and cloned from bovine pituitary follicular cells in 1989[8]. cDNA cloning revealed that there are four (major) isoforms of VEGF-A created by splicing, which include $VEGF_{121}$, $VEGF_{165}$, $VEGF_{189}$, and $VEGF_{206}$[9].

1.2 - Angiogenesis arises from existing vasculature.

Under normal, physiologic conditions, endothelial cells of the vasculature have very low turnover and rarely undergo mitosis[10]. While angiogenesis can occur in many settings, the formation of new blood vessels begins with new capillaries arising from the sprouting of small venules. Next, the basement membrane of the parent venule is degraded, and endothelial cells migrate towards the angiogenic stimulus. The migrating endothelial cells elongate and align with each other to form a solid sprout, with a lumen arising within each endothelial cell. Endothelial cell proliferation increases the length of the sprout, and two hollow sprouts merge at the tip to form a loop, which begins the flow of blood. Pericytes next position themselves at the base of the loop, and new sprouts can grow at the apex of the loop to continue the process of angiogenesis[1,11].

1.3 - A number of angiogenic factors have been discovered.

It is now known that a number of growth factors can induce angiogenesis *in-vitro* and *in-vivo*. The extent to how potently they can induce effects is highly variable, but some of these factors include bFGF, aFGF, EGF, PDGF, VEGF, Angiogenin, Angiotropin, TGF-β, TNF-α, G-CSF, and GM-CSF [12]. In the setting of cancer, these factors can be produced by the tumor cells themselves, mobilized from the extracellular matrix, or released by macrophages that have infiltrated the tumor. Despite the existence of multiple mechanisms by which a growth factor may induce tumor neovascularization, VEGF is the main factor responsible in primary, solid neoplasms[13].

1.4 - The VEGF family consists of multiple genes and receptors.

Initial cDNA cloning revealed that there are four (major) isoforms of VEGF created by splicing, which include $VEGF_{121}$, $VEGF_{165}$, $VEGF_{189}$, and $VEGF_{206}$[9]. It is now known that 4 VEGF genes exist: VEGF-A, VEGF-B, VEGF-C, and VEGF-D. There are also 3 different VEGF receptors, named VEGFR-1, VEGFR-2, and VEGFR-3[14]. VEGF-A is the major form of VEGF, and can bind to VEGFR-1 and VEGFR-2, whereas VEGF-B can only bind to VEGFR-1, and VEGF-C as well as VEGF-D can bind to both VEGFR-2 and VEGFR-3[14,15]. The different members of VEGF and their interactions with VEGF receptors are illustrated in Figure 2.

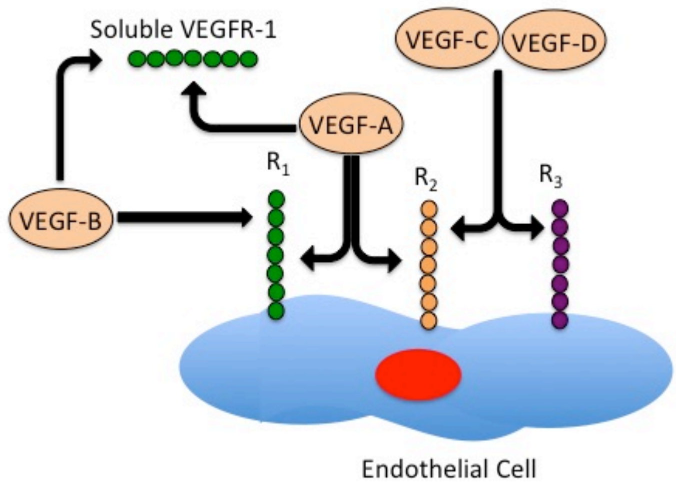

Figure 2: The Vascular Endothelial Growth Factor Family and its receptors. Adapted from Ferrara *et al* (2003).

The main isoform of VEGF-A is $VEGF_{165}$, which is a 45 kDa homodimeric glycoprotein that exerts the majority of its mitogenic, angiogenic, and permeability enhancing effects through VEGFR-2[9,16]. The effects of VEGFR-1 signaling are not fully understood, but is believed to play a role in the induction of matrix metalloproteinases and recruitment of macrophages to tumor vasculature which can play a role in the induction of angiogenesis[9,14,17]. As previously mentioned, VEGFR-1 is the only target for VEGF-B, and therefore it may play a role in these processes, but since it cannot signal through VEGFR-2, it is not responsible for predominant angiogenic effects. VEGF-C and VEGF-D regulate lymphangiogenesis[14-15].

VEGFR-1 also exists in a soluble form that may serve as a decoy for VEGF-A, or possibly as a method of VEGF sequestration[9]. In addition to the ability to bind to VEGFR-1 and VEGFR-2, VEGF-A can also bind to Neuropilin-1 (NP1) and Neuropilin-2 (NP2)[14]. Binding of $VEGF_{165}$ to NP1 has been shown to potentiate VEGFR-2 signaling, while NP1 also has the ability to directly bind VEGFR-1[17]. This suggests that VEGFR-1 may negatively regulate angiogenesis by competing for NP1 binding[9,14]. Furthermore, some tumors express NP1 and NP2 on their surface, although in the setting of tumor angiogenesis the significance of the neuropilin, VEGF, VEGF-R signaling pathway is still uncertain[17] Of note, the VEGF-A family member $VEGF_{165}$ is almost always referred to as simply “VEGF” in literature, and will subsequently be referred to likewise throughout the rest of the text unless otherwise indicated.

1.5 - VEGFR-2 is activated by $VEGF_{165}$ binding.

VEGFR-2 is a receptor tyrosine kinase that consists of seven immunoglobulin-like domains in the extracellular domain, a single transmembrane region, and a tyrosine kinase sequence that is interrupted by a kinase-insert domain[16]. VEGF binds to the second and third Ig-like domains, which induces VEGFR-2 dimerization and tyrosine auto-phosphorylation[9,14]. VEGFR-2 is predominantly expressed on endothelial cells of the vasculature, and while the effects of VEGFR-2 activation are numerous, in endothelial cells it results in the phosphorylation of phospholipase C-y, PI-3 kinase, Ras GTPase-activating protein, and Src family members[14,18].

1.6 - VEGF expression is regulated through multiple mechanisms.

It was first observed that tumors are often accompanied by extensive vascularity over a hundred years ago[7]. While the explanation for how and why was unknown for most of the 20th century, even after the discovery of VEGF it remained to be elucidated what induced its expression. VEGF production was initially observed to be induced by hypoxia and tissue ischemia[19]. The researchers found that in glioblastoma samples from cancer patients, levels of VEGF mRNA were correlated with proximity to centers of necrosis and ischemia. Furthermore, they demonstrated that growth of glioblastoma cells under hypoxic conditions resulted in a significant increase in VEGF expression, which was reversible upon re-exposure to normal oxygen levels.

In an attempt to elucidate the mechanism by which hypoxia induces VEGF expression, it was found that VEGF shared similar expression activity as erythropoietin[20]. It was later determined that a common enhancer exists for both VEGF and erythropoietin: a binding site for hypoxia inducible factor-1 (HIF-1) [21]. Although VEGF expression is regulated by HIF-1, it can be induced independently of low oxygen tension through mutations in PI3K/AKT and PTEN[22]. This is one mechanism by which tumor cells can hijack normal cellular regulatory mechanisms to produce VEGF and recruit blood vessels.

Cytokines and growth factors that do not directly induce angiogenesis can exert a pro or anti-angiogenic effect by modulating VEGF expression in specific cell types[23]. For example, FGF-4, PDGF, TNF-α, TGF-β, IL-1β and IL-6 can all induce VEGF production, along with hormones such as TSH and ACTH in responsive tissues[9,23]. It was previously mentioned that VEGFR-1 can serve as a method of sequestering VEGF, and macrophages have been shown to modulate angiogenesis through production of VEGFR-1[24]. In contrast, neutrophils have been shown to produce VEGF[25]. This evidence suggests that the immune system may play an active role in determining the extent to which angiogenesis occurs under both physiologic and pathologic conditions.

1.7 - The tumor microenvironment nurtures tumor growth.

The interaction between a primary tumor and cells of both the innate and adaptive immune system has been shown to play a fundamental role in determining the grade and malignancy of a tumor[26]. However, cancer cells do not only interact with myeloid and lymphoid cells, but numerous studies have shown they receive strong additional support from interactions with stromal cells, such as fibroblasts and angiogenic vascular cells[27,28,29]. These other cell types in the tumor microenvironment may play a role in deregulating cellular energetics, sustaining proliferative signaling, evading growth suppressors, inducing angiogenesis, avoiding immune destruction and activating invasion and metastasis[30]. For example, tumor-associated macrophages have been shown to promote breast cancer metastasis, suppress apoptotic signals, and provide protection from chemotherapeutic agents[30]. Inflammation, a prominent phenotypic expression of the immune system, has long been known to have an effect on either cancer progression or suppression. Tumor-associated inflammatory cells promote cancer cell proliferation and suppress antitumor immunity[31]. Inflammation acts as a mechanism for neovascularization, which can provide nutrients and serve as routes for metastasis[32]. This interaction between the primary tumor and secondary cells types is an area of intense active research.

1.8 - T-Lymphocytes are actively involved in tumor growth and suppression.

There is an increasing awareness that T-cells play a major role in the tumor microenvironment, especially the T_H17 subset of CD4+ T-cells. These cells are associated with both positive and negative outcomes among different tumor types in humans, including potentially anti-tumor effects in NHBL (Non-Hodgkins B-cell Lymphoma), prostate, ovarian, and breast cancers, while having potentially pro-tumor effect in gastric cancer, hepatocellular carcinoma, NSCLC (Non-Small Cell Lung Cancer), and melanoma[33,34]. Numasaki et al demonstrated that IL-17, the hallmark cytokine for T_H17 cells, has a significant effect on angiogenesis, promoting it through CXCR-2 in human NSCLC, while Chung et al showed that in mouse models of lymphoma, IL-17 promotes angiogenesis via a G-CSF, NF-kB, ERK signaling pathway[35,34]. These results demonstrate that IL-17 can promote tumor growth via multiple mechanisms, which could ultimately be the target of specific pharmacotherapy. Furthermore, increased numbers of interleukin-17 producing cells have been correlated with high grade and negative outcomes in breast carcinoma[26], while tumor infiltrating T_H17 cells are associated with poor outcomes in colorectal and lung carcinomas[36].

1.9 - T_H17 cells mediate effects via two different cytokines: interleukin-17 and interleukin-22.

Previous work has shown that Th17 cells promote tumor resistance to anti-angiogenic therapy[35]. The authors postulated that IL-17 mediates this effect, and showed IL-17 inhibition is sufficient to render tumors sensitive[35]. One group of researchers have suggested that IL-22 stimulates production of VEGF and Bcl-X_L[37]. Since T_H17 cells produce IL-17 and IL-22, this suggests that they mediate resistance to VEGF inhibition via IL-17, while stimulating VEGF production via IL-22. Furthermore, in cutaneous T-cell lymphoma, IL-22, but not IL-17, dominates within the tumor microenvironment[38]. Researchers are still uncertain why T_H17 cells promote tumor growth in certain tissues, but inhibit it in others. Many tumors do not express the IL-17 receptor, however, and thus IL-17 mediates its effects through other cell types in the tumor microenvironment, or the effects of T_H17 cells must be acting through a molecule other than IL-17[39,34]. Furthermore, T_H17 cells have even been found to be associated with both positive and negative outcomes in human breast cancer patients, suggesting that a particular mediator is responsible for this discrepancy[40,26]. The work that follows in chapters 2-4 arose from the notion that IL-22, the other primary T_H17 cell cytokine, could be responsible for the observations that T_H17 cells exhibit differential effects on tumor growth.

1.10 - Interleukin-22 is a T cell secreted cytokine in the IL-10 family.

Interleukin-22 is a cytokine that belongs to the IL-10 family. It is a 179 amino acid protein which is secreted as an alpha-helical molecule[41,42]. It was first discovered and isolated in 2000 from mouse T lymphocytes, and given the tentative name “IL-10 related T cell-derived inducible factor,” [43]. IL-22 shares 22% sequence homology with IL-10 in mice, and 25% sequence homology with IL-10 in humans[42,44].

Interleukin-22 interacts with the IL-22 receptor, a type-II cytokine receptor. The IL-22 receptor is a transmembrane protein dimer, which consists of an IL-22R1 and an IL-10R2 subunit[21]. The IL-10R2 chain is ubiquitously expressed in human tissues, while the IL-22R1 subunit is primarily localized to tissues of epithelial origin[45,46]. Although both subunits are capable of ligand binding, neither can transduce IL-22 signaling alone[46]. The IL-22 receptor complex contains binding sites for Janus tyrosine kinases (JAK), which become activated after ligand binding[47]. JAK then phosphorylates tyrosine residues of the receptor, which create docking sites for Src homology 2 binding proteins such as STATs[48].

IL-22 is largely considered to be a T-cell cytokine, although innate natural killer cells (large granular lymphocytes) can produce modest amounts[49,45]. Many studies investigating the role of IL-22 have taken place in the context of dermatologic pathologies, and psoriasis was the first disorder associated with abnormal IL-22 production, which derives from CD4+ T_H1,

T_H17, and T_H22 cells, whereas in atopic dermatitis IL-22 is derived primarily from T_H22 cells and CD8+ IL-22 producing cells[50]. Not all IL-22 activity is deleterious, however, as T_H derived IL-22 has been postulated to play a protective effect in patients with ulcerative colitis and Crohn's disease[50,51.]

The source of IL-22 varies among settings, although IL-6 and IL-23 have been shown to promote its production[52]. In humans, retinoic acid receptor related orphan receptor C (RORC) and aryl hydrocarbon receptor (AHR) are thought to positively regulate IL-22 expression[53]. In contrast, transforming growth factor Beta (TGF-β) inhibits IL-22 production by acting through the transcription factor c-Maf[54]. Maximal concentrations, ~1.2 ng / mL, of IL-22 are produced by CD4+ T-cells when stimulated with IL-6, and IL-23 can also stimulate production of IL-22, but in lower concentrations[55].

1.11 - Role of Interleukin-22 in the epithelium and on the endothelium

IL-22's effect on epithelial cells has been well documented. Rutz et al (2013) and Sabat et al (2014) provide thorough reviews and background on the role of IL-22 in both the normal epithelium and pathologic states[56,50]. Briefly, its primary physiologic role is to promote barrier defense against pathogens at mucosal surfaces and promote wound healing as well as tissue homeostasis. Overproduction of IL-22 is observed in many human disease states, which is well summarized in Sabat et al (2014).

Investigations into the role of IL-22 on the endothelium, however, are far more limited. IL-22 has been shown to affect endothelial cells at the blood-brain barrier, namely resulting in inflammation[57]. During the course of the following investigations, a group of researchers showed that IL-22 can inhibit apoptosis in pulmonary microvascular endothelial cells[58]. Another group demonstrated that IL-22 can promote HUVEC proliferation, and enhance their barrier function by reducing permeability[59]. As such, it is increasing recognized that interleukin-22 can have a direct effect on the vasculature.

1.12 - Angiogenesis plays a major role in tumor growth.

Angiogenesis has long been known to play a major role in cancer growth. Solid tumors can receive nutrients and exchange waste while they are small, but to grow beyond 1-2mm in size, they must recruit new blood vessels for these processes to occur [5]. Furthermore, many believe it is the rate-limiting factor for rapidly dividing tumor cells[35]. Numerous studies have shown the link between endothelial stimulation via Vascular Endothelial Growth Factor (VEGF) and cancer progression. Anti-angiogenic therapy, when combined with chemotherapy, has been clinically proven to increase survival in patients with advanced malignancies[60].

Although the anti-VEGF monoclonal antibody bevacizumab improves clinical outcome in a number of cancers, patients exhibit a heterogeneous response[61]. This observation in clinical trials has led to a number of follow-up investigations into predictive biomarkers, but ultimately none of them have been prospectively validated[61,62]. Many of the clinical trials for which anti-VEGF therapy has shown therapeutic benefit have been in the setting of advanced malignancies. Therefore it is possible that earlier adjuvant therapy may yield valuable information for which patients will receive greatest benefit from anti-angiogenic therapy, as well as lend insight to the mechanisms by which tumors develop resistance[63]. Much work has yet to be done in elucidating interactions within the tumor microenvironment that help or hinder anti-angiogenic treatment, and furthermore, which patients will benefit most from such therapy[17].

It was previously discussed how the immune system plays an active and important role in the tumor microenvironment. Anti-angiogenic therapy in particular can promote leukocyte infiltration into tumors[64]. In contrast, IL-22 blockade has been shown to reduce granulocyte infiltration[65]. Additionally, IL-22 reduces T_H2 cell production of IL-4, a potent anti-tumor cytokine, which further suggests that interleukin-22 can exhibit a pro-tumor effect [41,66]. Hence it is possible that IL-22 may play a role in mediating resistance to anti-VEGF therapy. This could arise from directly acting on the endothelium to induce angiogenesis, or perhaps through effects on cells of the innate immune system, with the endothelium as both a mediator and final target in the process. The following chapters attempt to elucidate some of the effects interleukin-22 has in the settings of angiogenesis and tumor growth.

CHAPTER 2.

Effects of Interleukin-22 on Endothelial Cells

2.1 - Introduction

Interleukin-22 is known to exert a direct effect on epithelial cells. IL-22 is unusual among interleukins in this regard, as epithelial cells are major targets of the IL-22 ligand, whereas interleukins traditionally serve as mediators for inducing effects on immune cells[50]. IL-22's physiological role is in mediating host defense, and overproduction of IL-22 is associated with many disease conditions such as psoriasis, inflammatory bowel disease, and asthma[50]. Although IL-22 has been found to exhibit multiple effects on epithelial cells, hepatocytes, and pancreatic cells, its ability to act on endothelial cells is only beginning to be elucidated[56].

2.2 - Results

2.2.1 - Endothelial cells express IL-22 receptor on their cell surface.

Although IL-22 receptor expression has been well documented in epithelial cells, it was necessary to confirm that the available endothelial cells indeed expressed the IL-22 receptor on the cell surface. Utilizing HepG2 as a positive control, a western blot demonstrated positive staining for IL-22 receptor in both HUVEC and MVEC cells (Figure 3). Protein isolation from these cells requires cell lysis, and thus it is conceivable that the cells produce IL-22 receptor, but it is not necessarily transported to and functional on the cellular surface. To address this, HUVEC, MVEC, and HepG2 cells were incubated with a fluorescent antibody against IL-22 receptor or an IgG isotype control antibody. Live cells were then analyzed using flow cytometry (Figure 4). With HepG2 as a positive control, both HUVECs and MVECs demonstrated increased mean fluorescence intensity with IL-22 receptor antibody staining compared to isotype control. This increase in fluorescence signaling was statistically significant across the three cell types analyzed. Although this experiment included an isotype control antibody was as a technical control, HepG2 cells were next incubated with multiple doses of a siRNA against IL-22R to ensure that the observed FACS staining for IL-22R was specific. This specificity could be determined by reduced IL-22 receptor fluorescence staining following targeted knockdown. siRNA treatment reduced surface staining for IL-22R in HepG2 cells (Figure 5). This served as a final confirmation that the fluorescence staining observed following incubation with anti-IL22 receptor antibody was indeed specific. In summation, these findings suggest that the IL-22R is expressed on the surface of endothelial cells.

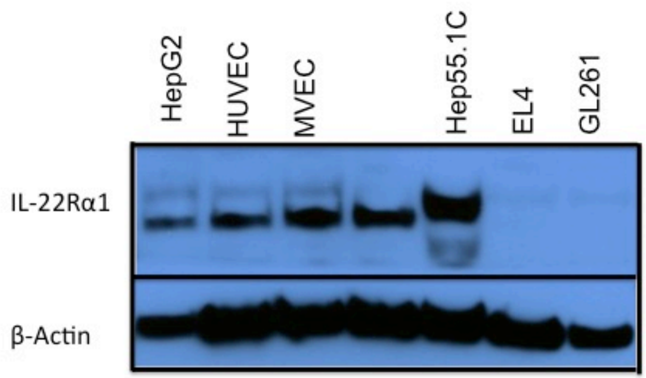

Figure 3: Human IL-22 Receptor Expression. Representative Western Blot shows that both HUVEC and MVEC express the IL-22Rα1 subunit

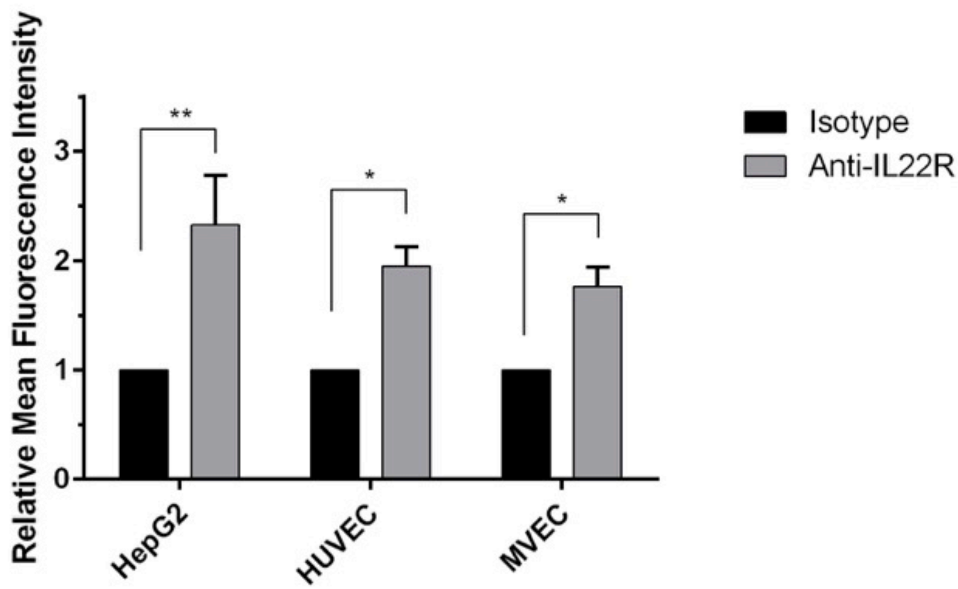

Figure 4: Human IL-22 Receptor Surface Staining By Flow Cytometry. (error bars indicate standard deviation, n = 2, ** p < .01, * p < .05 by two-way ANOVA with post-hoc Šidák's correction for multiple comparisons)

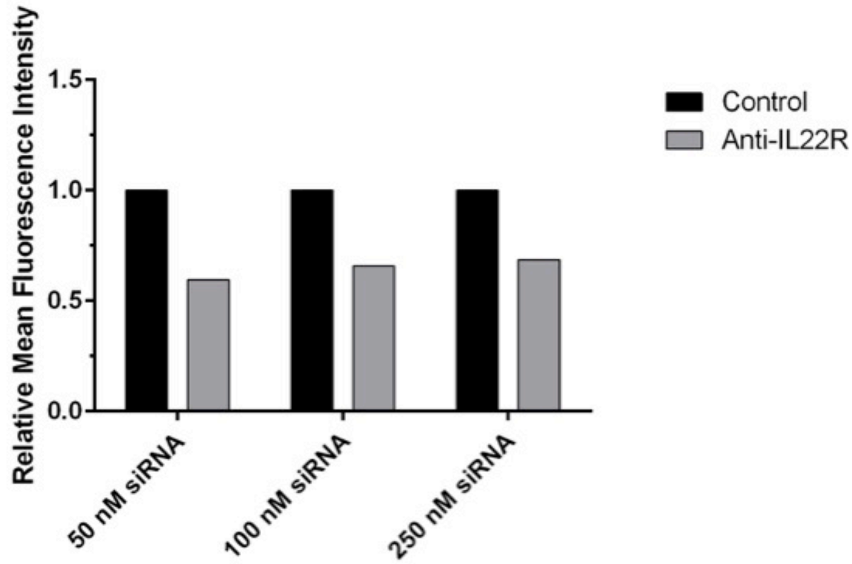

Figure 5: siRNA Knockdown of Human IL-22 Receptor. Relative IL-22R fluorescence following single oligonucleotide siRNA knockdown (control siRNA or one targeting IL-22Rα1), assessed by flow cytometry.

2.2.2 - Endothelial Cell numbers are increased following IL-22 treatment.

He et al demonstrated that treating HUVECs with IL-22 caused an increase in proliferation[59]. It was independently observed that 3-day incubation of HUVECs with IL-22 results in increased cell numbers compared PBS control (Figure 6). When 2.5×10^4 cells were plated, the PBS control resulted in approximately double the number of cells present after 3 days. In contrast, IL-22 treatment resulted in over four times the number of cells present compared to the initial plating. This data demonstrates that IL-22 has a direct effect on increasing the proliferation of HUVECs.

Having observed a proliferation function of IL-22 on HUVECS, it was next examined whether IL-22 treatment could increase HUVECS survival. Increasing doses of IL-22 demonstrated a modest, but statistically significant pro-survival effect on HUVECs (Figure 7).

Having demonstrated that IL-22 could directly act on HUVECs, MVECs were investigated as another endothelial cell line to determine if the effects observed are common amongst different types of endothelial cells. Increasing doses of IL-22 failed to result in increased cell numbers following 3 day incubation (Figure 8). While basal media supplemented with 10% FBS produced a statistically significant increase in cell numbers compared to PBS control, IL-22 treatment did not. This suggests that in MVEC, IL-22 does not directly promote proliferation as observed in HUVECs.

Ren et al showed that IL-22 increases MVEC survival. A similar observation was found following a 6-day treatment of IL-22 (Figure 9). VEGF and bFGF treatment resulted in cell numbers 10-20 fold higher than media alone or PBS control. IL-22 incubation, in comparison, produced cell numbers approximately 5 fold higher than media alone or PBS treatment. Hence although IL-22 did not increase the number of MVECs in a proliferative fashion, it can increase cell number through survival mechanisms.

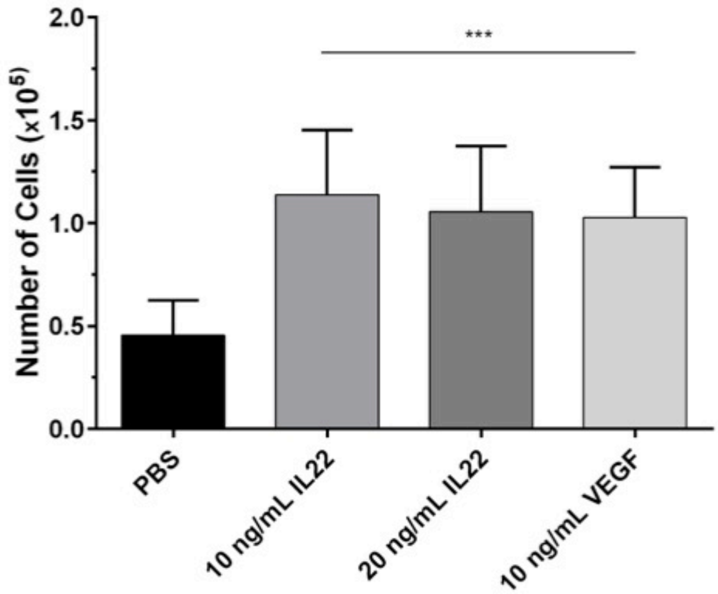

Figure 6: IL-22 Promotes HUVEC Proliferation. (error bars indicate standard deviation, n = 18, *** p < .001 by one-way ANOVA with post-hoc Dunnett's test for multiple comparisons)

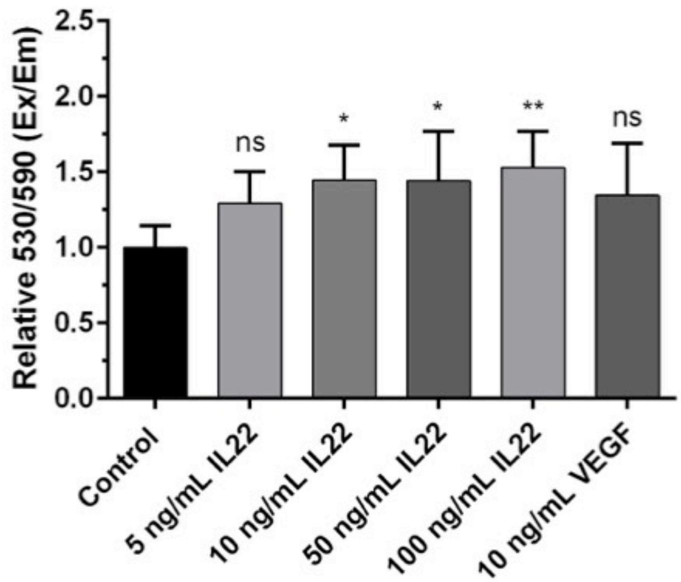

Figure 7: IL-22 Promotes HUVEC Survival. Assessed by alamar blue viability assay. (error bars indicate standard deviation, n = 6-8, * p < .05, ** p < .01, *** p < .001 by one-way ANOVA with post-hoc Dunnett's test for multiple comparisons)

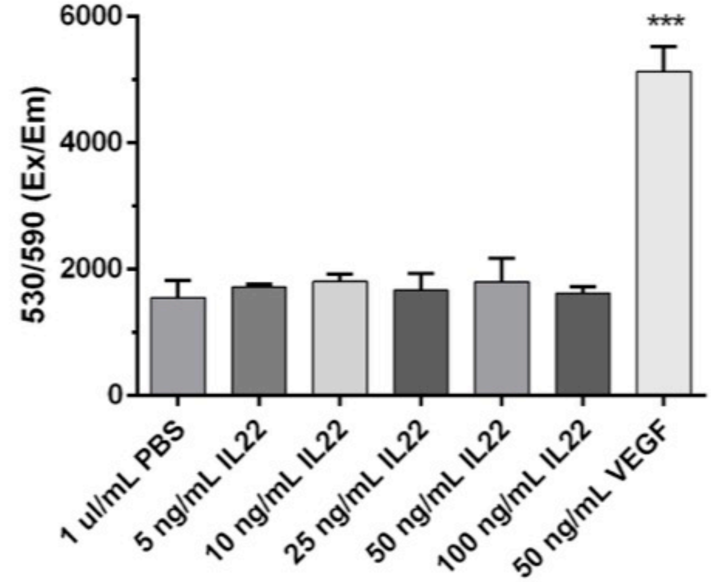

Figure 8: IL-22 Does Not Promote MVEC Proliferation. Assessed by alamar blue viability assay. (error bars indicate standard deviation, n = 2, *** p < .001 by one-way ANOVA with post-hoc Dunnett's test for multiple comparisons)

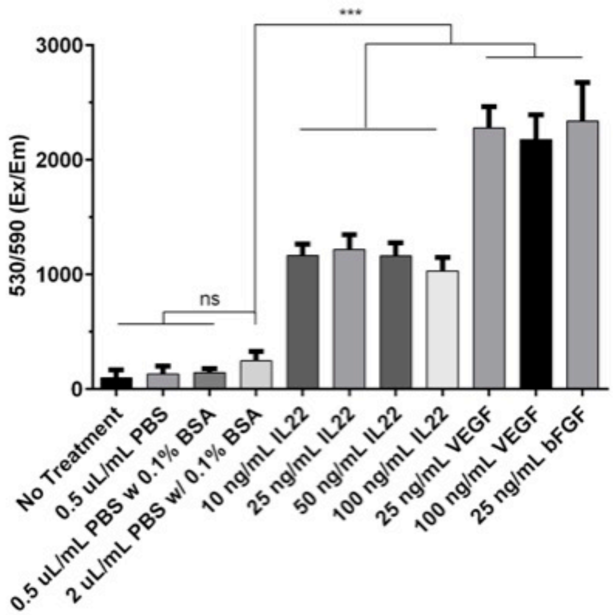

Figure 9: IL-22 Promotes MVEC Survival. Assessed by alamar blue viability assay. (error bars indicate standard deviation, n = 8, *** p < .001 by one-way ANOVA with post-hoc Dunnett's test for multiple comparisons)

2.2.3 - IL-22 promotes endothelial cell chemotaxis

Although endothelial cell proliferation and survival play a role in angiogenesis, vessel sprouting is another response that endothelial cells can exhibit in the presence of stimuli. Cell migration across a transwell membrane serves as a functional assay to determine chemoattractant potential of cytokines[67]. To determine if IL-22 could elicit such an effect on endothelial cells, a boyden chamber was utilized as previously described[68]. With HUVECs, compared to PBS, it was observed that IL-22 causes a 50-100% increase in migrated cell number (Figure 10). This suggests that IL-22 can directly promote endothelial cell migration and has a chemoattractant effect on endothelial cells. The role of IL-22 on cellular migration was also investigated with MVEC (Figure 11). Again, IL-22 demonstrated the ability to increase the number of cells that migrate across a transwell membrane. This suggests that IL-22 can directly stimulate endothelial cell chemotaxis, which could play a role in angiogenesis in-vivo.

Another functional angiogenesis assay to investigate the angiogenic potential of a cytokine is the tube formation assay[69]. In this assay, endothelial cells are plated atop a layer of solidified basement membrane extract. Media is added containing cytokines, and at a specified time later, the number and size of tubes that form can be ascertained. Using HUVECs, a low dose of IL-22 (10 ng / mL) increased the relative area of the tubes that formed (Figure 12).

Interestingly, higher doses of IL-22 resulted in smaller tubes, and were not statistically different from PBS control.

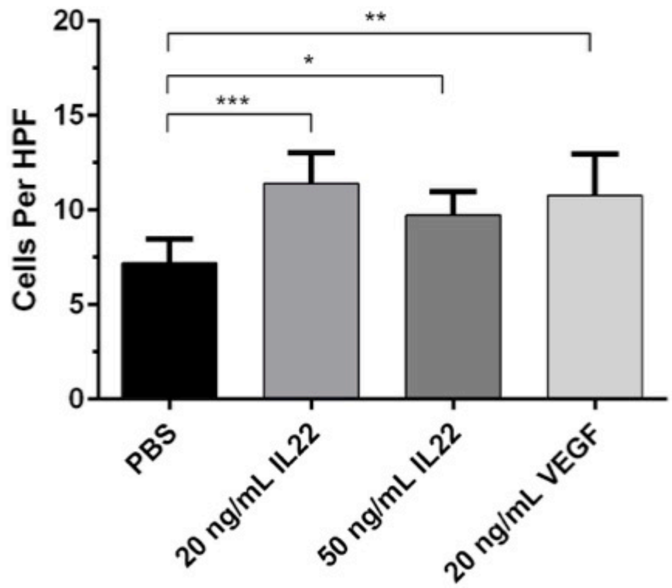

Figure 10: IL-22 Promotes HUVEC Migration. Representative of 3 independent experiments (error bars indicate standard deviation, n = 6, * p < .05, ** p < .01, *** p < .001 by one-way ANOVA with post-hoc Dunnett's test for multiple comparisons)

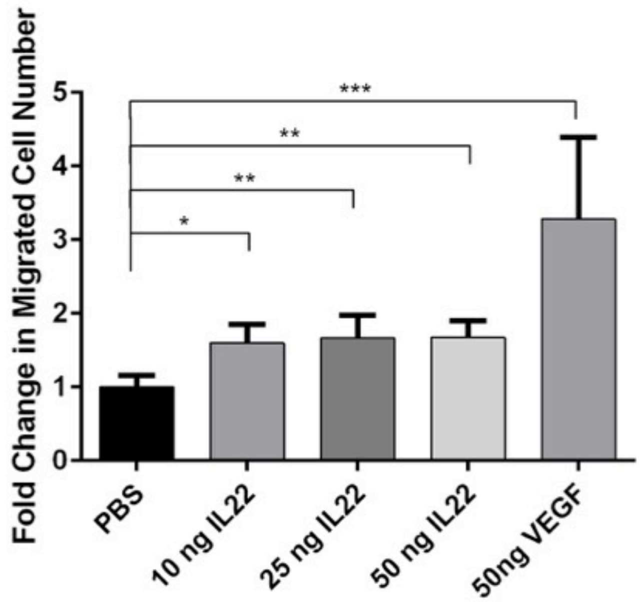

Figure 11: IL-22 Promotes MVEC Migration. Representative of 2 independent experiments (error bars indicate standard deviation, n = 4, * $p < .05$, ** $p < .01$, *** $p < .001$ by one-way ANOVA with post-hoc Dunnett's test for multiple comparisons)

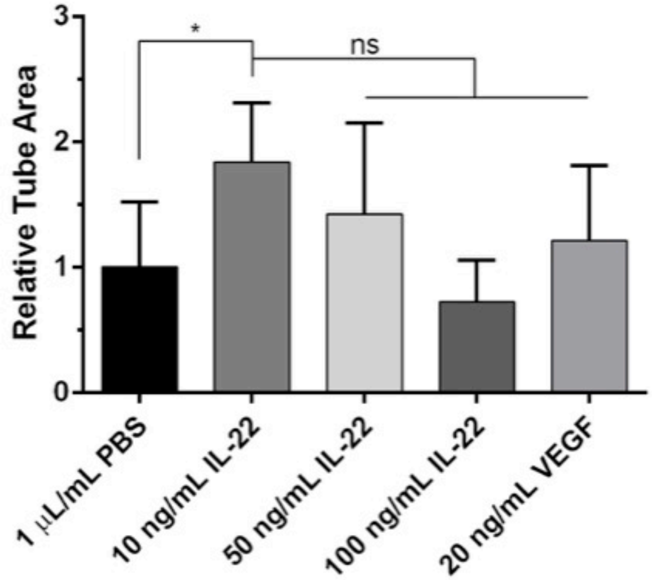

Figure 12: IL-22 Induces Tube Formation in HUVEC. (error bars indicate standard deviation, n = 5, * p < .05 by unpaired Welch's t-test)

2.2.4 - Signaling induced by IL-22 in endothelial cells

Having observed the effects of IL-22 on endothelial cell viability and chemotaxis in-vitro, it was next examined which signaling pathways are activated by IL-22 treatment. In HUVECs, initial experiments revealed that ERK 1/2 had markedly increased phosphorylation following 30 minute incubation with IL-22, with maximal effect between 10 and 25 ng / mL (Figure 13). An increased range of IL-22 concentrations was investigated, and a dose-dependent effect on ERK 1/2 activation was observed up until 100 ng / mL of IL-22 (Figure 14). Repeat examination with doses of IL-22 ranging from 1 to 500 ng / mL demonstrated peak relative ERK 1/2 activation at 25 ng / mL (Figure 15).

IL-22 can signal through the AKT pathway in HUVECs (Figure 16). After 30-minute stimulation, maximal p-AKT was observed with 25 ng/mL IL-22 treatment. A broader range of IL-22 doses were tested, and p-AKT measured following 10 and 30-minute incubations (Figures 17-18). Of note, the levels of activation observed relative to PBS control are lower than those previously observed. It is unclear whether this relates to use of 12-well versus 6-well dishes, or is partially due to the relative variation induced by loading smaller volumes of lysate into gels containing more lanes, and hence lower volumes.

IL-22 stimulation was also found to induce STAT 3 phosphorylation (Figure 19). Quantification of p-STAT 3 revealed increasing activation from 10 to 25 to 50 ng / mL of IL-22. HUVECs were also treated with 25 ng/mL of IL-

22, and cell lysates collected at different time intervals to assess its effect on STAT 3 phosphorylation over time. It was observed that IL-22 causes activation at 10 minutes, with relatively stable activation across 30, 60, and 120-minute time points (Figure 20).

In summation, this signaling data suggests that IL-22 appears to promote a combination of both pro-survival and proliferative pathways in endothelial cells.

A

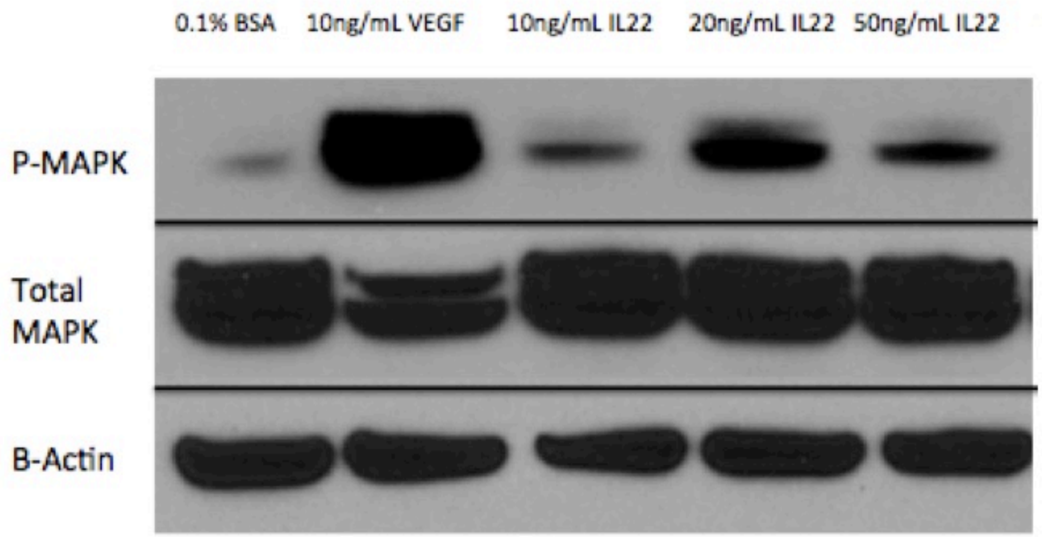

B

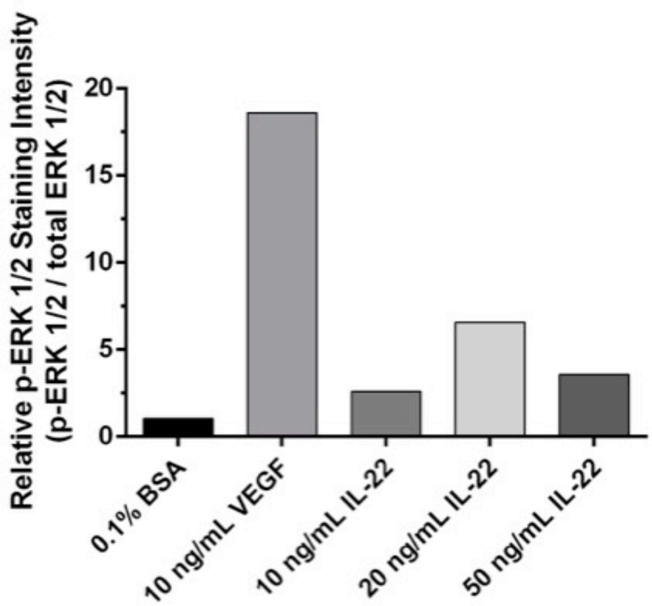

Figure 13: Quantification of p-ERK 1/2 Induced by IL-22. **A.** Western Blot staining after 10 minute incubation. **B.** Quantification of p-ERK 1/2 Induced by IL-22.

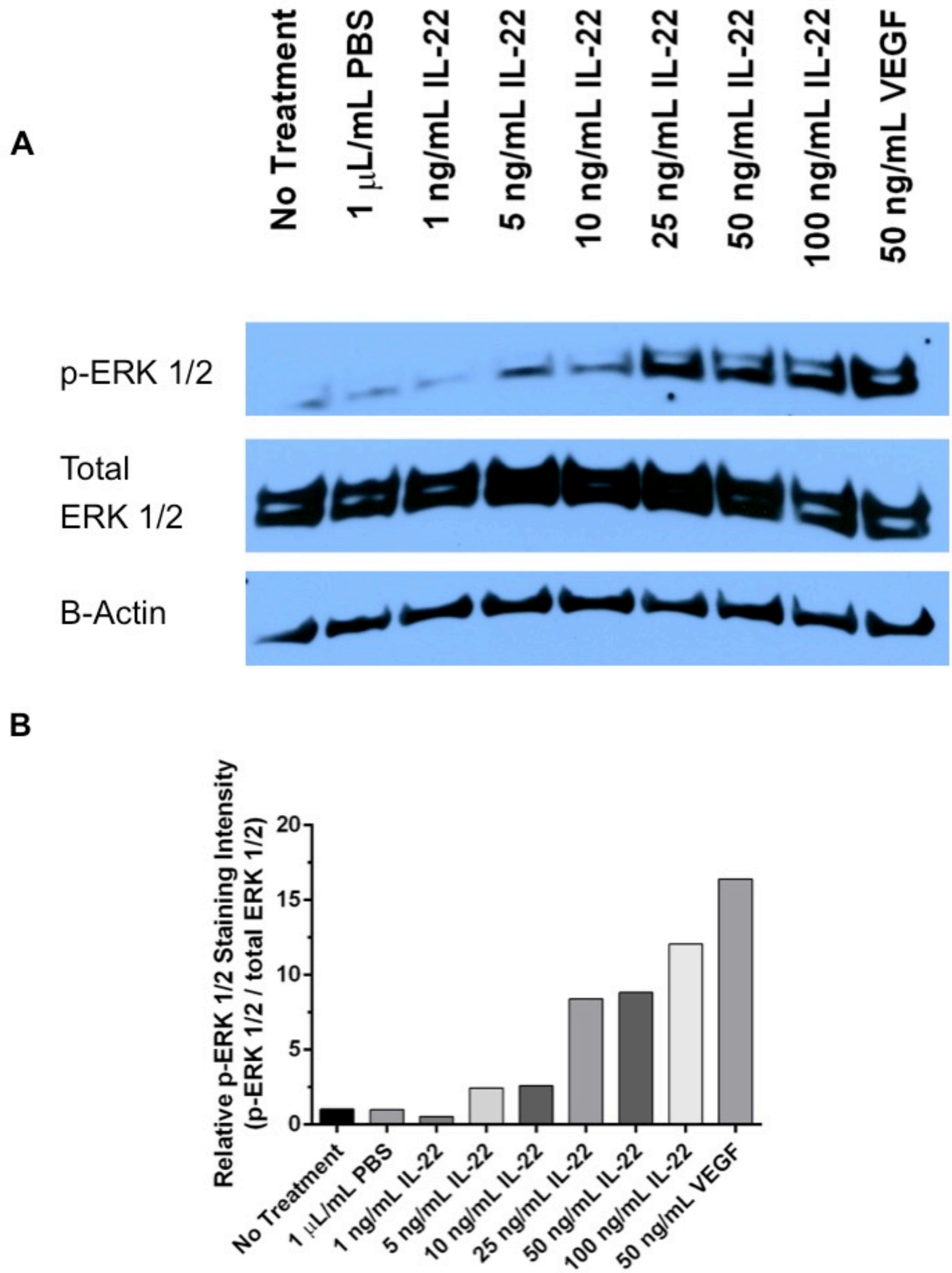

Figure 14: IL-22 Induces MAPK Activation in HUVEC. **A.** Western Blot staining after 30 minute incubation. **B.** Quantification of p-ERK 1/2 compared to total ERK 1/2.

A

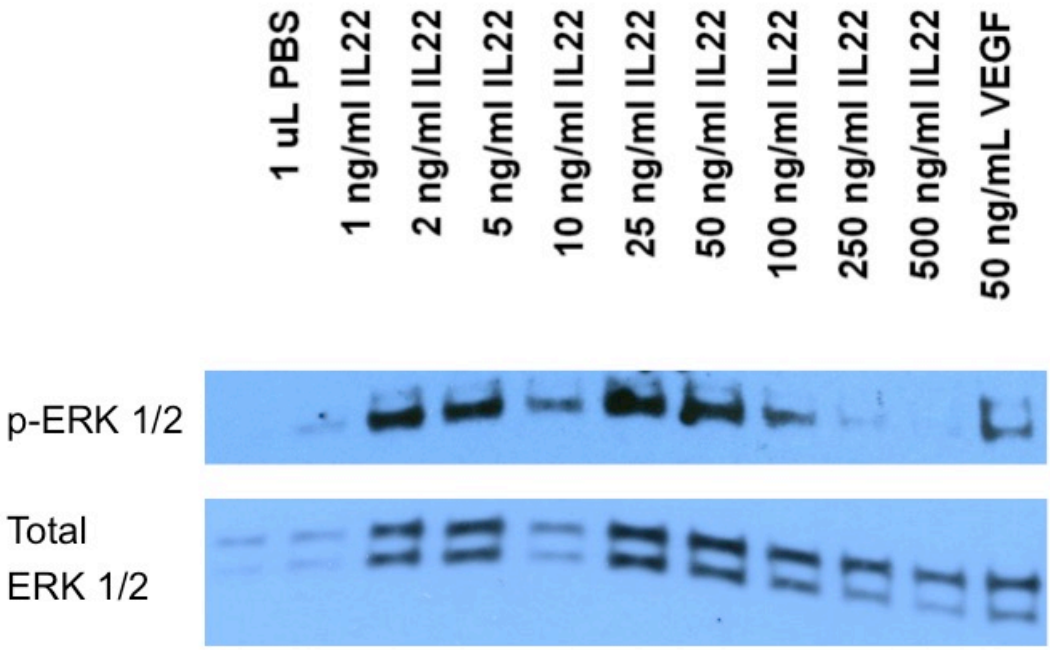

B

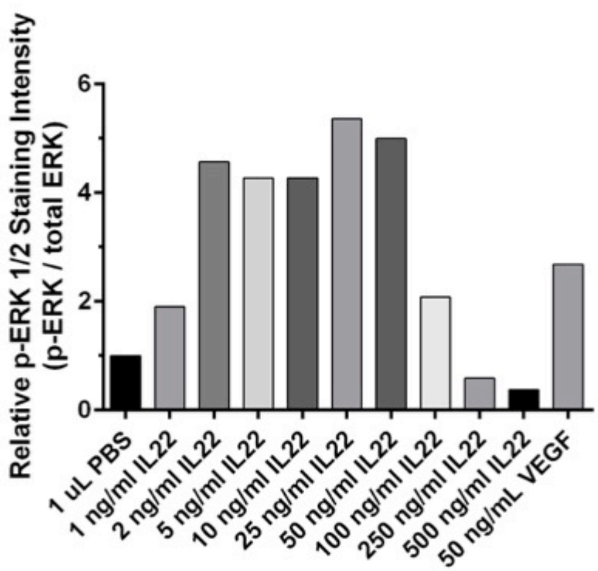

Figure 15: IL-22 Induces ERK 1/2 Activation in HUVEC. **A.** Western Blot staining after 30 minute incubation. **B.** Quantification of p-ERK 1/2

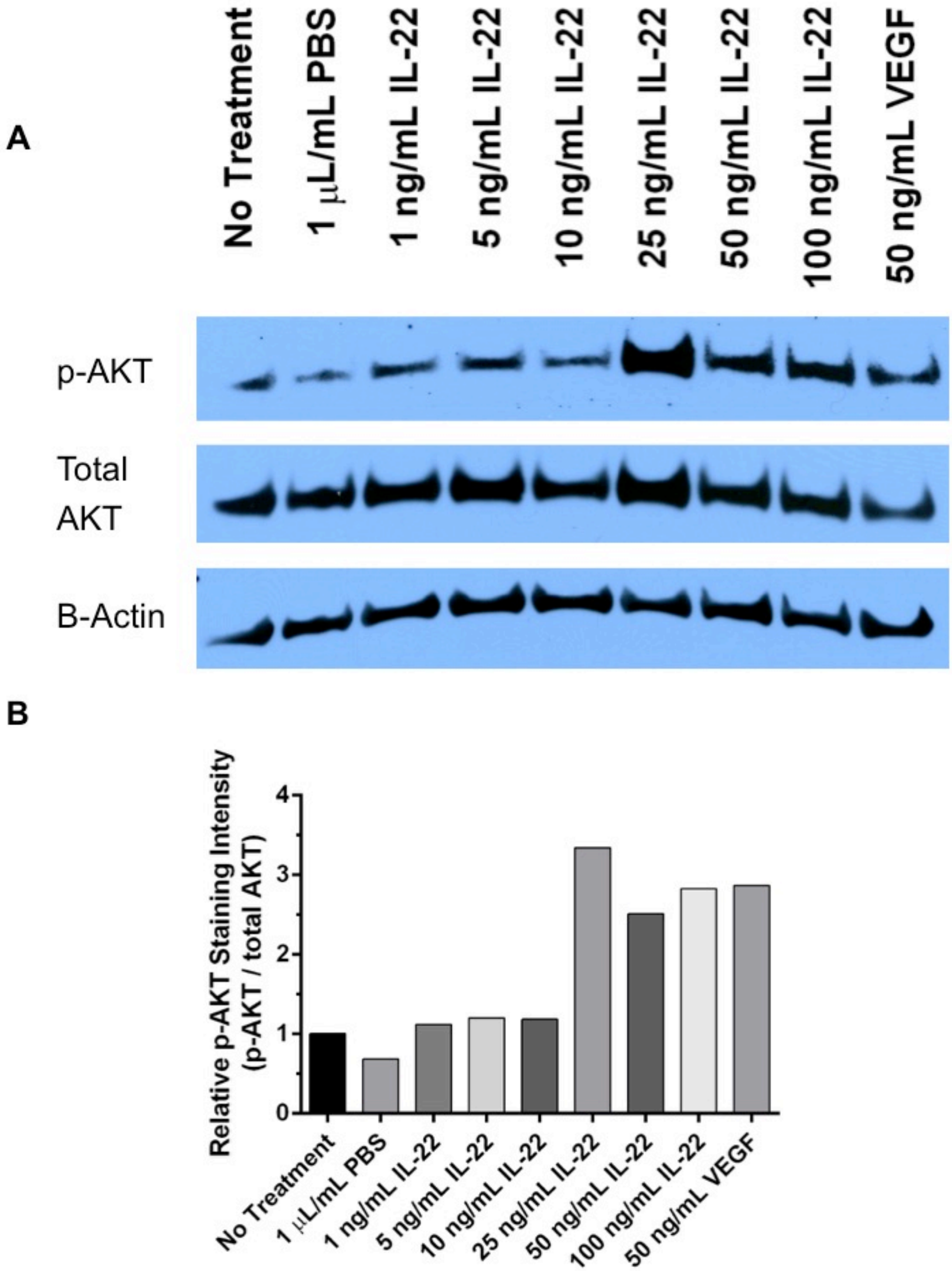

Figure 16: IL-22 Induces AKT Activation in HUVEC. **A.** Western Blot staining after 30 minute incubation. **B.** Quantification of p-AKT.

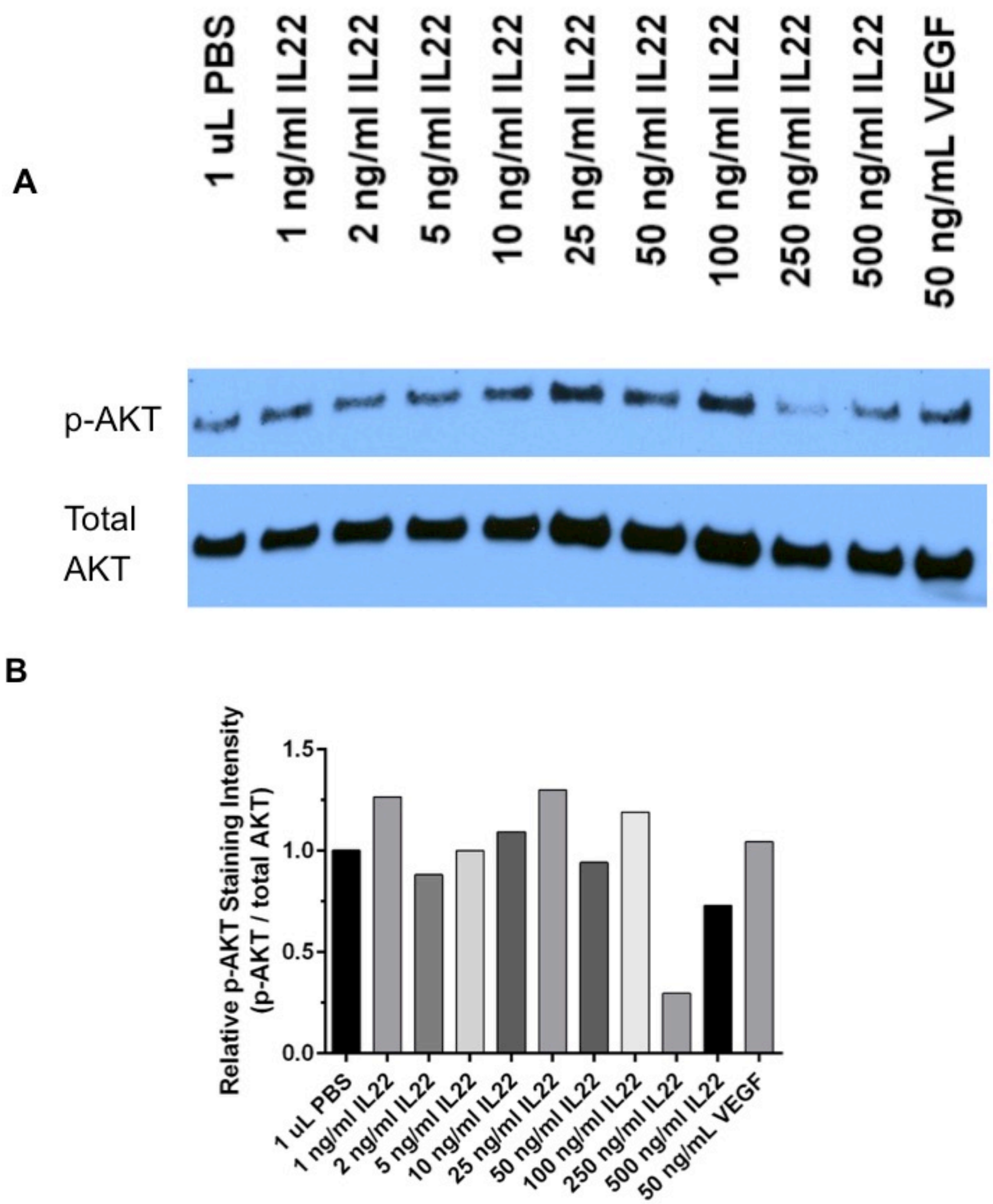

Figure 17: IL-22 Induces AKT Activation in HUVEC. **A.** Western Blot staining after 10 minute incubation. **B.** Quantification of p-AKT.

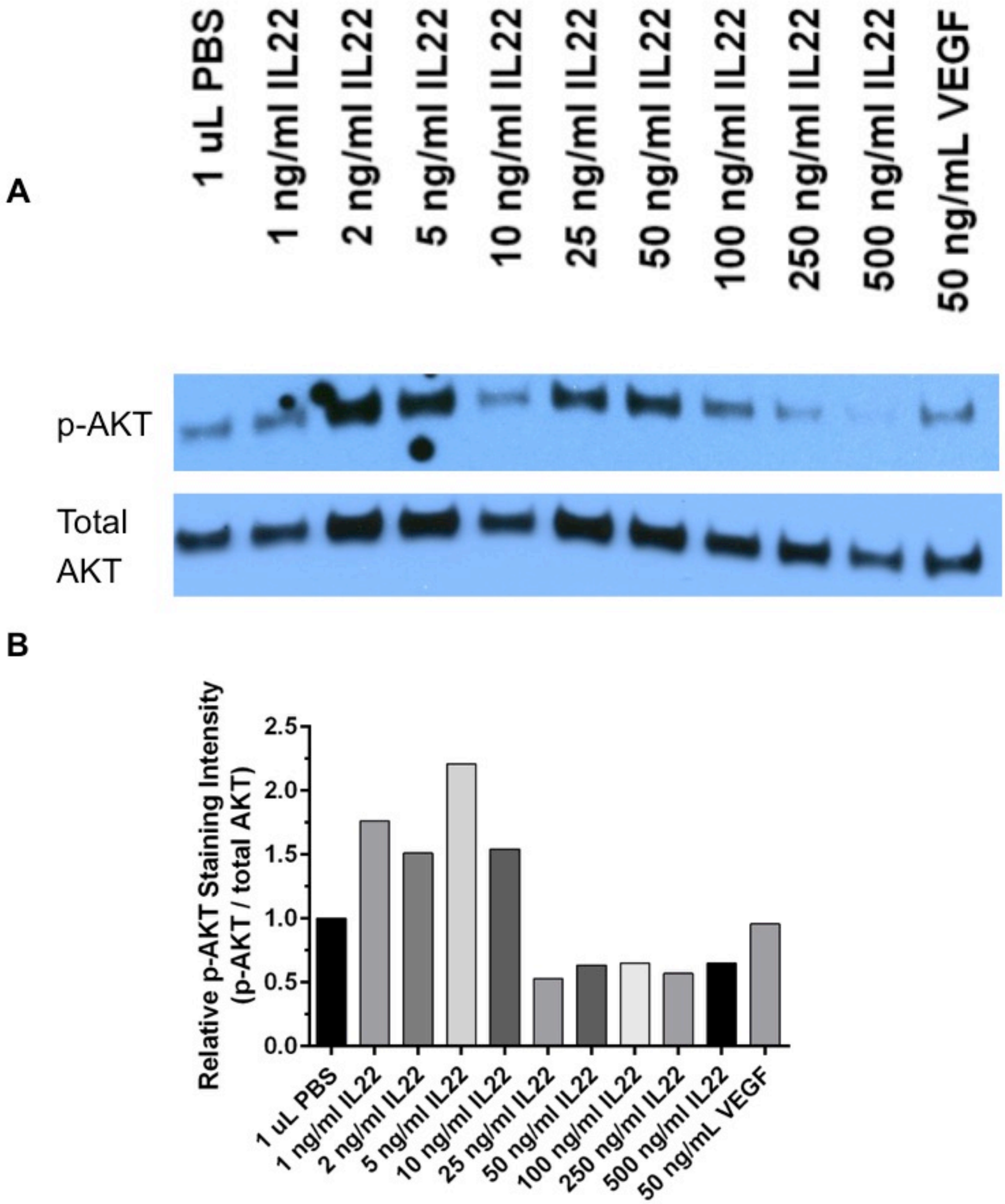

Figure 18: IL-22 Induces AKT Activation in HUVEC. **A.** Western Blot staining after 30 minute incubation. **B.** Quantification of p-AKT

A

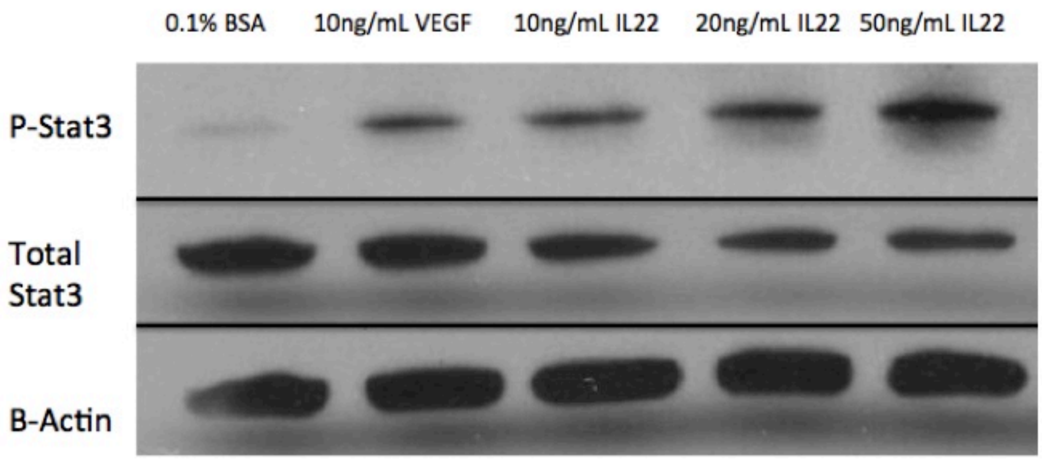

B

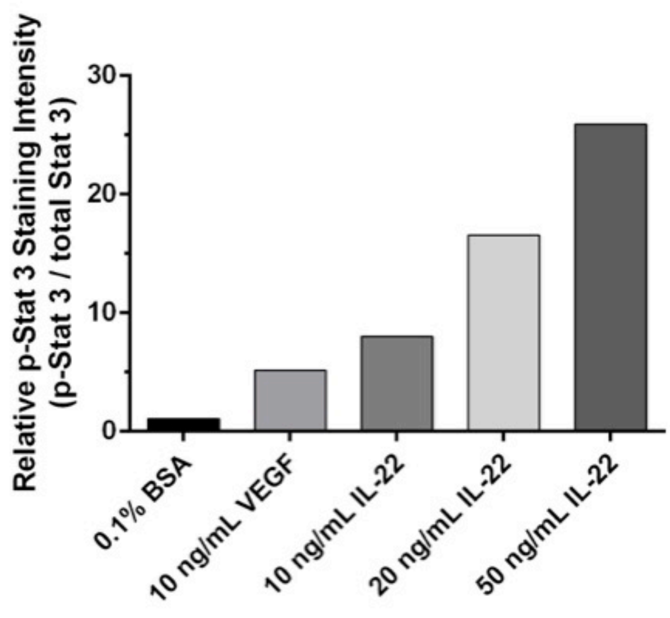

Figure 19: IL-22 Induces Stat 3 Activation in HUVEC. **A.** Western Blot staining after 30 minute incubation. **B.** Quantification of p-Stat 3 Induced by IL-22.

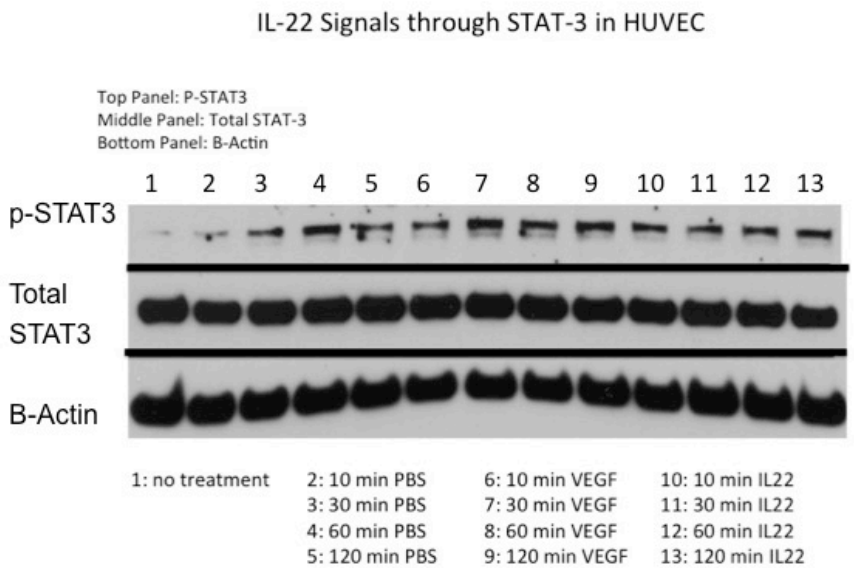

Figure 20: Stat 3 Activation Over time in HUVEC. Representative Western Blot shows that treatment with IL-22 results in increased p-Stat 3 staining at multiple time points.

2.3 - Discussion

It is well-established in the field of immunology that IL-22 can directly act on epithelial cells, but IL-22's effects on endothelial cells are only beginning to be investigated. It was found that IL-22 can elicit a proliferative and survival effect in HUVECs. In MVEC, IL-22 can promote survival, but not proliferation. Common to both cell types was the effect of inducing migration in a transwell assay. HUVECs, as their name implies, are derived from the umbilical cord, whereas the MVECs utilized in this study were isolated from adult lungs. It is possible that inherent differences exist in the downstream pathways between these cell types such that HUVECs are more responsive to stimuli compared to MVECs. IL-22 has been shown to be elevated in patients with asthma, and may even have a protective effect in the setting of lung inflammation and injury[50,70]. If IL-22 is indeed protective in the setting of lung inflammation, it could explain why MVECs exhibit some, but not all of the results observed with HUVECs. Specifically, IL-22 was found to promote MVEC survival but not proliferation, despite the ability of IL-22 to promote both in HUVECs. While VEGF also promoted both survival and proliferation in MVECs, there are numerous human tissues that contain detectable levels of VEGF in normal physiologic, non angiogenic states[71]. It has been postulated that in these settings, VEGF may contribute to vessel homeostasis, even though VEGF is well-known to potently induce angiogensis[14]. Therefore in the case of lung endothelial cells, it is not unprecedented for a growth factor to promote cell or vessel survival, while not specifically inducing cellular proliferation.

It is also conceivable that as being derived from a specific patient, susceptibility of MVECs to IL-22 varies between different persons, and possibly as a function of age. While an interesting notion, the focus of this study was the role of interleukin-22 in tumor growth and angiogenesis, although it is certainly an avenue for further study.

In the case of HUVECs, it appears that IL-22 promotes its canonical signaling pathways, including but not limited to MAPK, STAT3, and AKT. STAT3 is known to promote growth and survival[72]. Hence IL-22 promoting HUVEC proliferation and survival is consistent with the phosphorylation of STAT3 observed following IL-22 treatment. The MAPK and STAT3 pathways are known to act synergistically in the setting of interleukin-22 treatment[73]. As a result it can be difficult to discern which downstream effects are due exclusively to one signaling cascade versus another, even in the presence of pharmacologic inhibition. The data observed, however, demonstrates that IL-22 induces known effector signaling pathways in HUVECs, and thus there is likely conservation of many of IL-22’s effects on epithelial cells within the endothelial subset.

VEGFA was used extensively as a positive control for determining the angiogenic effects of interleukin-22. As expected, VEGF potently induced

HUVEC and MVEC proliferation, survival, and migration. VEGFR-2 (Flk-1) is agreed to be the major VEGF receptor responsible for the effects of VEGFA in endothelial cells[14]. As a receptor tyrosine kinase (RTK), VEGFR-2 has intrinsic kinase activity that results in autophosphorylation and activation after ligand binding and dimerization[14,74]. RTKs such as VEGFR-2 contain SRC-homology 2 domains that can signal through extensive, often overlapping pathways that include ERKs, AKT, and STATs, among many other intracellular mediators[75].

In contrast, the IL-22R is a type-II cytokine receptor that requires dimerization of the IL-22R1 and IL-10R2 subunits after ligand binding. The kinases JAK1 and TYK2 are associated to the cytoplasmic portions of the IL-22R1 and IL-10R2 subunits respectively[50]. In the case of the IL-22R1 subunit, STAT3 is associated with the cytoplasmic chain before IL-22 ligand binding and receptor dimerization, which allows for rapid phosphorylation by JAK1, P-STAT3 dimerization, and translocation to the nucleus[47,50]. IL-22 is known to induce STAT, MAPK, and AKT pathways, the activation of which were observed in HUVECS, but importantly, IL-22 has been shown in multiple studies to activate JAK1, but not JAK2[73,76]. Cytokine receptors are known to exhibit “cross-talk,” and JAK2 in particular has been shown to activate EGFR independently of ligand binding[77,78]. Given that IL-22 does not activate JAK2, it is possible that IL-22 signaling induces a more narrow range of downstream effectors compared to RTKs such as VEGFR-2. Furthermore, JAK1 is absolutely essential for IL-22 signaling[73]. This implies that although TYK2 is activated by IL-22, it is contingent on JAK1, and that subsequent STAT3 phosphorylation is the major mediator of IL-22 signaling. These functional characteristics could explain differences observed between IL-22 and VEGF in both signaling by western blot analysis, and using *in-vitro* assays.

Chapter 2, in part, is currently being prepared for submission for publication of the material. Protopsaltis, N.; Liang, W.; Nudleman, E.; Ferrara, N. The dissertation author was the primary investigator and author of this material.

CHAPTER 3.

Effects of Interleukin-22 in an EL4 Tumor Model

3.1 - Introduction

EL4 cells are a T-cell lymphoma on the C57BL/6 background, and as observed in multiple types of T-cells, EL4 cells are able to produce IL-22[79]. Multiple conditions were ultimately tested to determine the extent to which EL4 cells can produce IL-22 *in-vitro*, and to confirm previous reports that IL-22 can not directly affect cells of hematopoietic origin[56]. A major aim of this investigation was to determine the effects of inhibiting IL-22 on tumor growth. As such, EL4 was an aptly suited model since the cells were postulated to produce IL-22 *in-vivo* as well as not be directly inhibited by IL-22 blockade.

3.2 - Results

3.2.1 - EL4 cells do not express the IL-22 receptor

It has been reported that hematopoetic cells do not express the IL-22Rα1 subunit[45,56,80]. A western blot confirmed that EL4 cells do not stain for IL-22R (Figure 21). Hep55.1C, a mouse hepatocellular carcinoma cell line, served as a positive control to ensure that this lack of protein staining was not due to decreased species affinity of the antibody, but was indeed a lack of IL-22 receptor expression. It was important to show that EL4 cells lack this receptor, as EL4 expression of the IL-22R could affect cell growth with either addition or blockade of IL-22 *in-vitro*.

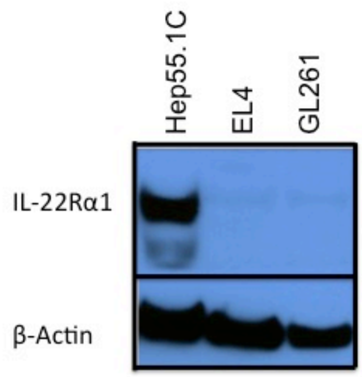

Figure 21: Mouse IL-22 Receptor Expression. Representative Western Blot shows that neither EL4 nor GL261 express the IL-22Rα1 subunit.

3.2.2 - Neither addition nor blockade of IL-22 affects EL4 growth *in-vitro*

To examine the effects of IL-22 in tumor angiogenesis, it was first necessary to ensure that IL-22 did not have a direct effect on EL4 cells themselves. Adding IL-22 to EL4 cells in culture did not result in an increase in cell number after 6 days, determined by an alamar blue cell viability assay (Figure 22). Doses from 5 ng/mL failed to increase cellular proliferation compared to PBS control, whereas cells plated in the presence of 10% FBS resulted in approximately 3 times greater cell number at endpoint compared to PBS control.

Given the observation that increased FBS promoted EL4 cell proliferation, varying doses of IL-22 were added with media containing either 0, 1, or 2% FBS. Regardless of media FBS content, IL-22 concentrations ranging from 5 – 100 ng / mL did not increase cellular proliferation (Figure 23).

The use of EL4 as a model system to investigate the role of IL-22 in tumor growth and angiogenesis ultimately requires administration of an anti-IL22 antibody. Although IL-22 did not increase EL4 proliferation *in-vitro*, it was necessary to ensure that IL-22 antibody blockade would not directly inhibit EL4 cell growth, as this could confound the effects of the antibody blockade on EL4 tumor growth *in-vivo*. Increasing doses of anti-IL-22 antibody did not result in decreased cell growth compared to IgG1A antibody treatment after 6 day incubation (Figure 24).

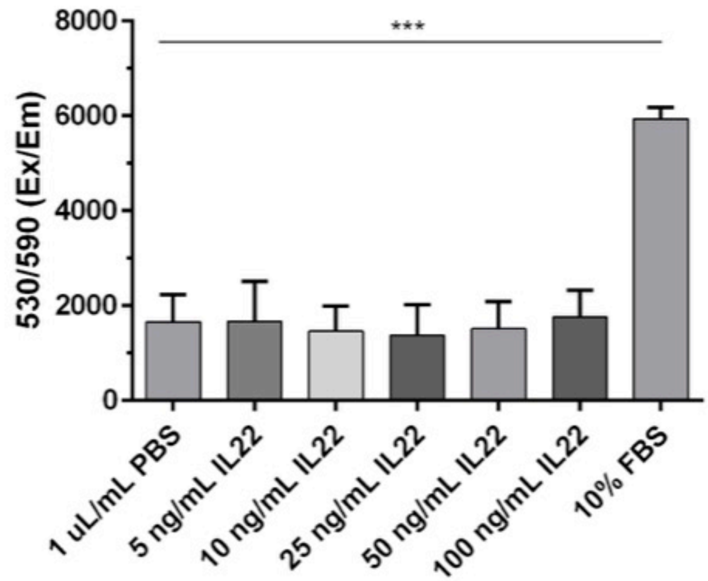

Figure 22: IL-22 Does Not Promote EL4 Proliferation. Assessed by alamar blue viability assay . (error bars indicate standard deviation, n = 2, *** p < .001 by one-way ANOVA with post-hoc Dunnett's test for multiple comparisons)

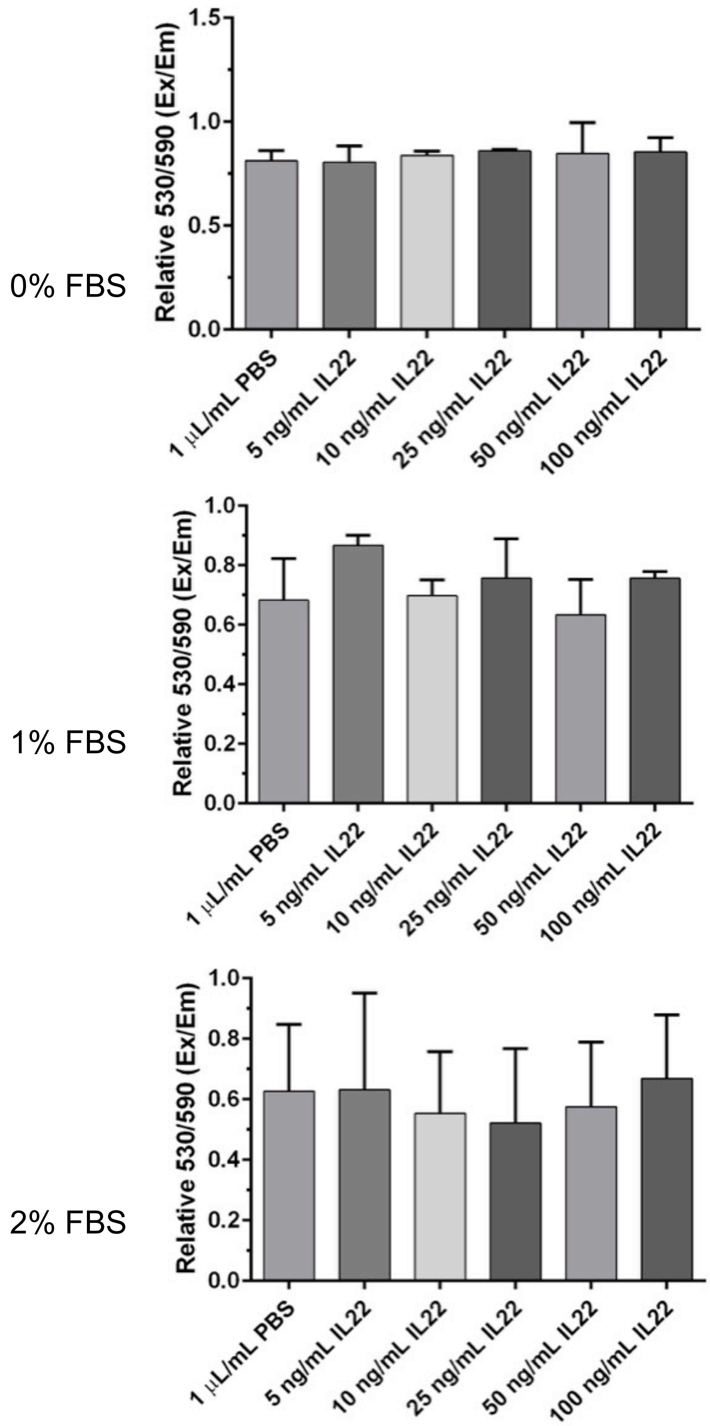

Figure 23: Increasing Serum Concentration Does Not Rescue IL-22 Independent EL4 Proliferation. Assessed by alamar blue viability assay. (error bars indicate standard deviation, n = 2, differences not significant by one way ANOVA with post-hoc Dunnett's test for multiple comparisons)

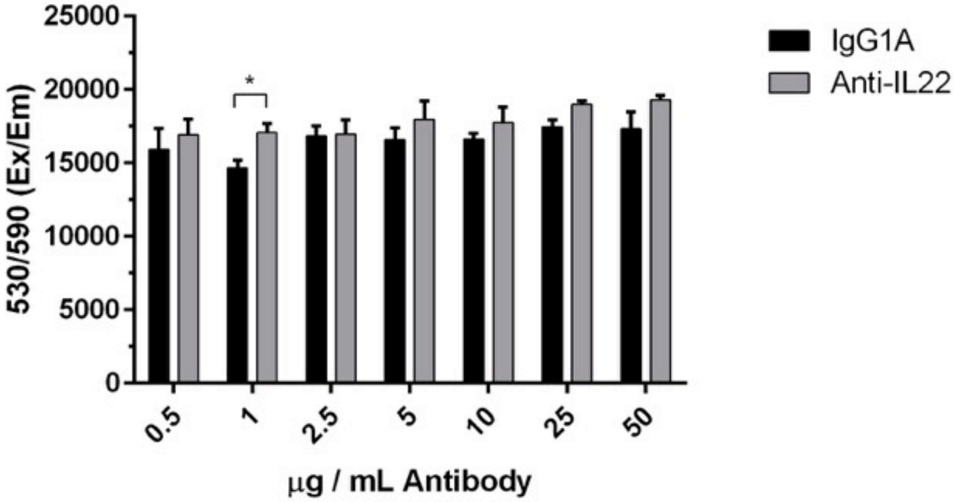

Figure 24: Anti-IL22 Antibody Does not Inhibit EL4 Growth in Vitro. Assessed by alamar blue viability assay. (error bars indicate standard deviation, n = 3, * p < .05 by two way anova with post-hoc Bonferroni correction for multiple comparisons)

3.2.3 - Anti-IL22 antibody treatment reduces EL4 tumor growth *in-vivo*

After ensuring that the blockade of IL-22 would not directly inhibit the growth of EL4 cells, they were injected into the flanks of C57BL/6 mice. Administration of anti-IL22 antibody resulted in a statistically significant decrease in tumor growth compared to IgG1A isotype control antibody treatment (Figure 25). Repeat study with a wider range of antibody concentrations demonstrated a dose-dependent effect of anti-IL22 antibody treatment on inhibiting EL4 tumor growth in C57BL/6 mice (Figure 26).

After observing the effects of IL-22 on endothelial cells, it was conceivable that IL-22 and VEGF could be acting synergistically to enhance tumor growth. To address this possibility, anti-IL22 and anti-VEGF combination therapy were given to EL4 tumor bearing mice, and it was observed that while combination treatment resulted in the greatest reduction in tumor growth compared to isotype control, the combination therapy did not result in a statistically significant difference compared to either therapy alone (Figure 27). Furthermore, ELISA analysis on these tumors revealed that the mice treated with anti-VEGF monotherapy had higher levels of IL-22 compared to those treated with anti-IL22 monotherapy (Figure 28). While it appears that anti-VEGF therapy increased tumor levels of IL-22, one-way ANOVA lacked the statistical power to find a significant difference.

Rag1$^{-/-}$ mice lack any functional T-cells, and therefore any significant contribution of IL-22 within the tumor microenvironment would have to be derived from the syngeneic tumor graft. EL4 cells were injected in $Rag1^{-/-}$ mice, and as previously observed in C57BL/6 mice, anti-IL22 antibody treatment resulted in a statistically significant decrease in tumor growth compared to treatment with isotype control antibody (Figure 29). A repeat study with a larger number of mice in each treatment group yielded the same conclusion (Figure 30). In this second batch of EL4 bearing $Rag1^{-/-}$ mice, tumors were collected at day 11 and those treated with anti-IL22 and anti-VEGF antibody were found to have a statistically significant decrease in weight compared to those treated with isotype control (Figure 31). These same tumors were stained with antibodies against CD31b, and those treated with anti-IL22 antibodies had a significant decrease in both the percent area of the tumor that was positively stained (Figure 32), as well as the number of vessels staining within the tumor (Figure 33).

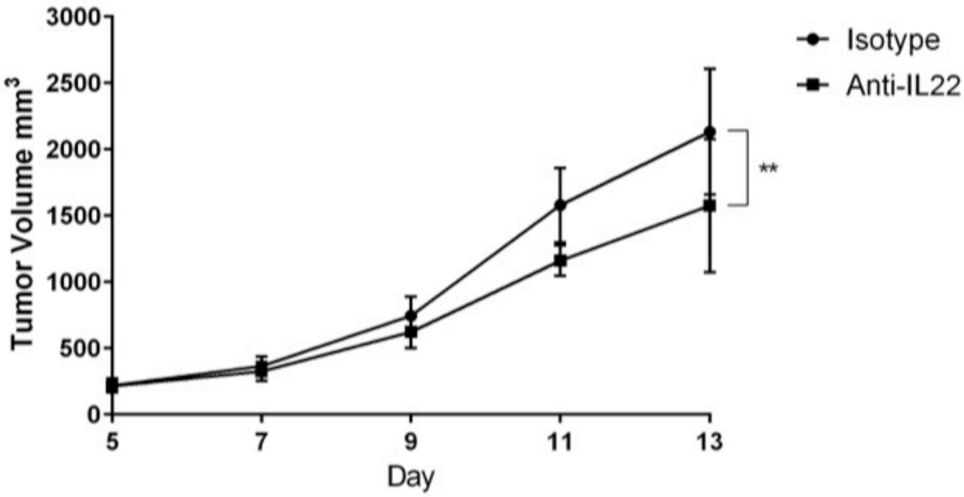

Figure 25: Anti-IL22 Antibody Treatment Reduces EL4 Tumor Growth in C57BL/6 Mice. (error bars indicate standard deviation, n = 5, ** $p < .01$ by two-way ANOVA with post-hoc Šidák's correction for multiple comparisons)

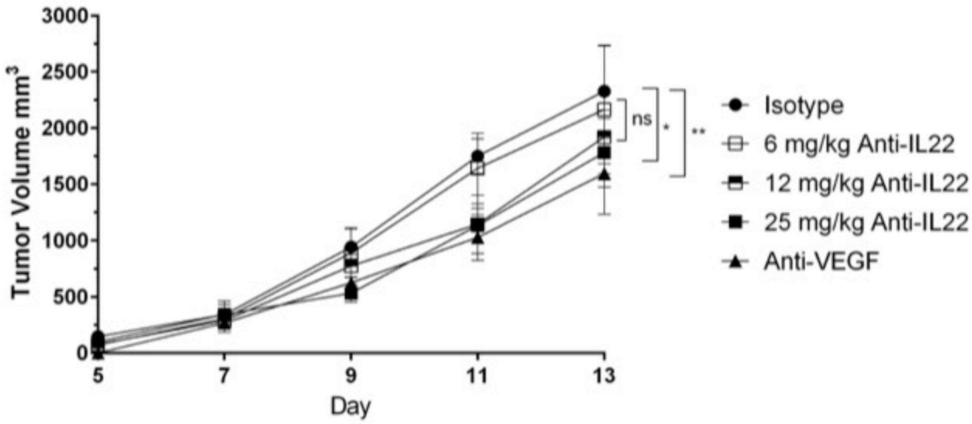

Figure 26: Anti-IL22 Antibody Treatment Demonstrates a Dose-Dependent Reduction in EL4 Tumor Growth in C57BL/6 Mice. (error bars indicate standard deviation, n = 5, ns = not significant, * $p < .05$, ** $p < .01$ by two-way ANOVA with post-hoc Tukey's test for multiple comparisons)

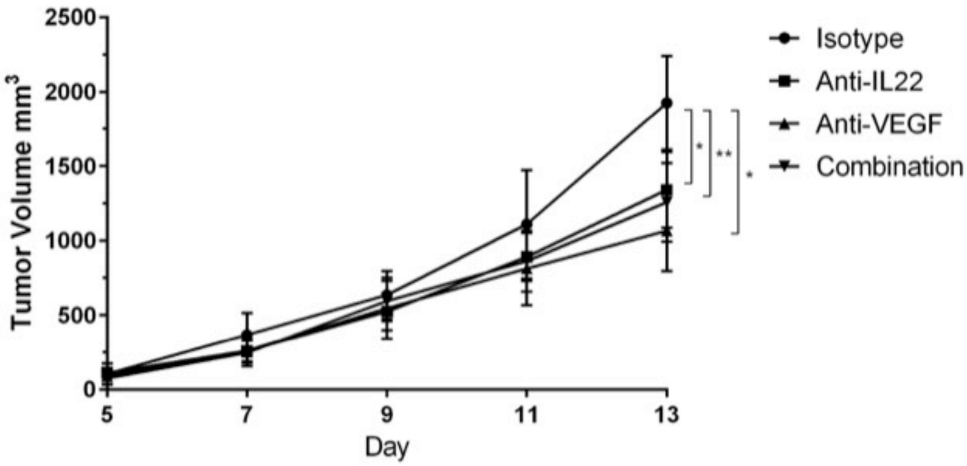

Figure 27: Combination Anti-IL22 and Anti-VEGF Antibody Treatment Reduces EL4 Tumor Growth in C57BL/6 Mice. (error bars indicate standard deviation, n = 8, * $p < .05$, ** $p < .01$ by two-way ANOVA with post-hoc Tukey's test for multiple comparisons)

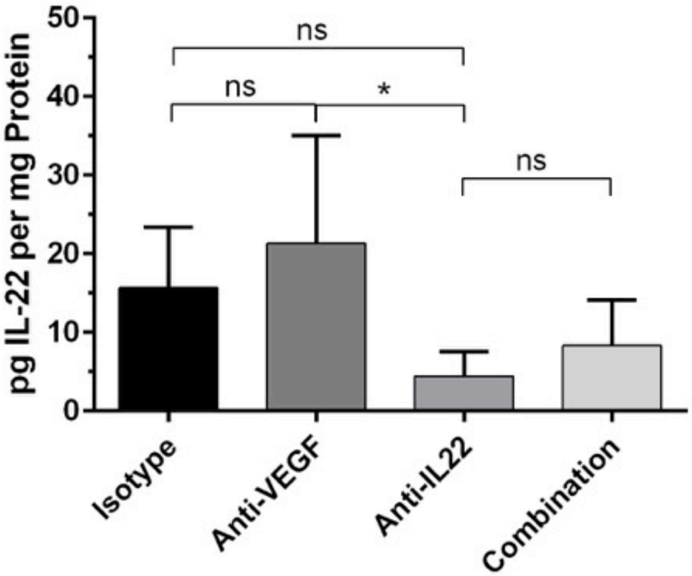

Figure 28: Anti-IL22 Treatment Reduces EL4 Tumor IL-22 Levels in C57BL/6 Mice. Assessed by ELISA. (error bars indicate standard deviation, n = 6, ns = not significant, * p < .05 by one-way ANOVA with post-hoc Tukey's test for multiple comparisons)

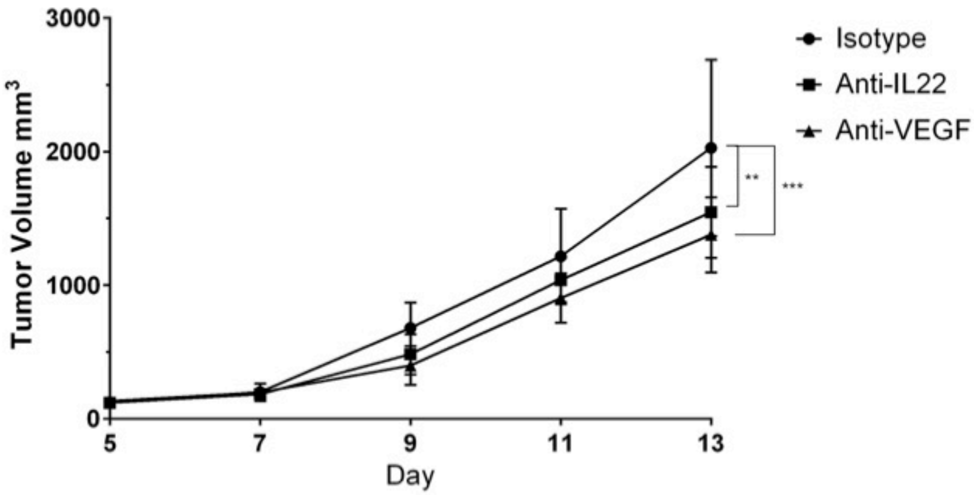

Figure 29: Anti-IL22 Antibody Treatment Reduces EL4 Tumor Growth in Rag1$^{-/-}$ Mice. (error bars indicate standard deviation, n = 5, ** $p < .01$, *** $p < .001$ by two-way ANOVA with post-hoc Tukey's test for multiple comparisons)

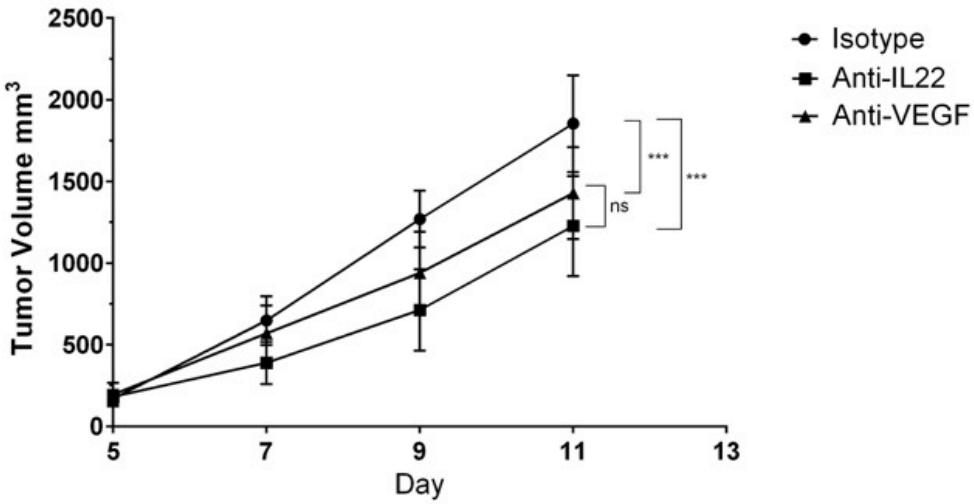

Figure 30: Anti-IL22 Antibody Treatment Reduces EL4 Tumor Growth in Rag1$^{-/-}$ Mice. (error bars indicate standard deviation, n = 9 - 10, ns = not significant, *** $p < .001$ by two-way ANOVA with post-hoc Tukey's test for multiple comparisons)

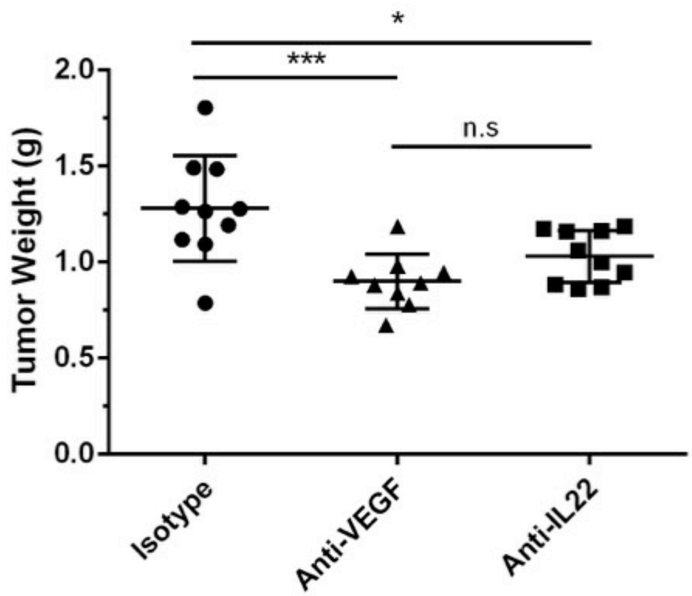

Figure 31: Anti-IL22 Antibody Treatment Reduces EL4 Tumor Weight at Endpoint in Rag1$^{-/-}$ Mice. (error bars indicate standard deviation, n = 9 - 10, ns = not significant, * p < .05, *** p < .001 by one-way ANOVA with post-hoc Tukey's test for multiple comparisons)

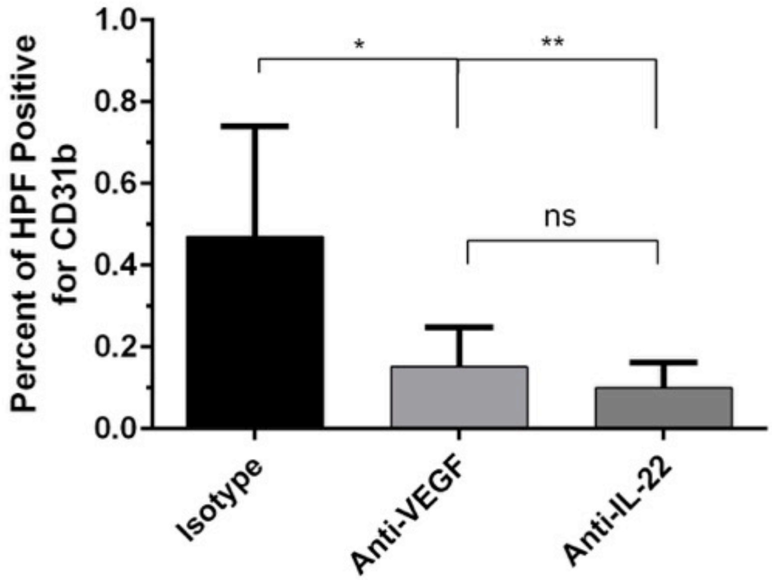

Figure 32: Anti-IL22 Antibody Treatment Reduces CD31b Staining in EL4 Tumors From Rag1$^{-/-}$ Mice. (error bars indicate standard deviation, n = 5, ns = not significant, * p < .05, ** p < .01 by one-way ANOVA with post-hoc Dunnett's test for multiple comparisons)

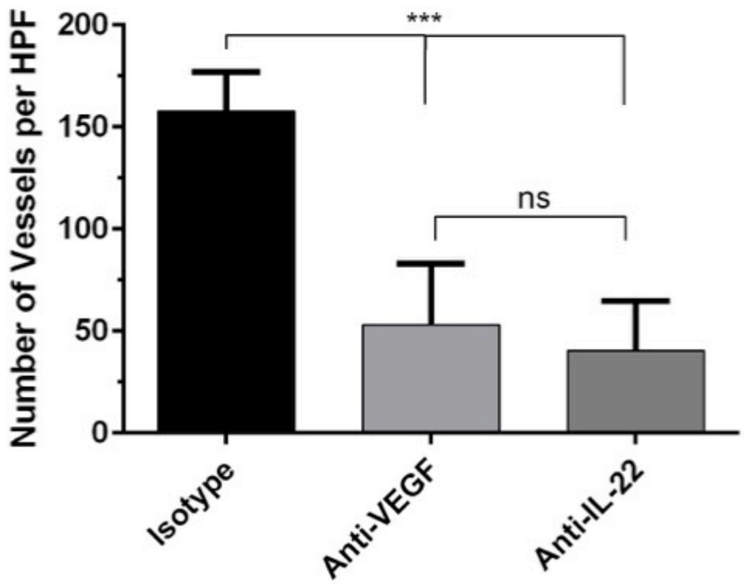

Figure 33: Anti-IL22 Antibody Treatment Reduces The Number of CD31b Staining Vessels in EL4 Tumors From Rag1$^{-/-}$ Mice. (error bars indicate standard deviation, n = 5, ns = not significant, *** p < .001 by one-way ANOVA with post-hoc Dunnett's test for multiple comparisons)

3.2.4 - CRISPR-Cas9 knockout of IL-22 ligand in EL4 cells

The primary reason the T-cell lymphoma EL4 was initially chosen to investigate the role of IL-22 in tumor growth and angiogenesis is that T-cells can produce IL-22. It was found that EL4 cells *in-vitro* can produce IL-22 levels over 1 μg/mL when stimulated with IL-6 and TGFβ (Figure 34). Although production is much smaller without any stimulation, hypoxic culture also greatly enhances IL-22 production.

A CRISPR-Cas 9 knockout transfection and sorting yielded a number of viable clones, which were stimulated and assayed by ELISA for IL-22 production (Figure 35). Selected clones were again stimulated and had their conditioned media concentrated 10 fold, which was then assayed by ELISA for IL-22 (Figure 36). The media produced from clones for IL-22 ligand KO numbers 3 and 10 were found to completely lack detectable levels of IL-22. Additionally, while the media used to culture these cells contains 10% FBS, the concentrated media also did not demonstrate any IL-22 reactivity in the ELISA assay. The FBS is bovine in origin, and despite species specific reactivity of the IL-22 ELISA, it is conceivable that there could be some cross-reactivity, especially given the very high protein content in the concentrated media. This experiment, however, assuaged any concerns that the FBS containing media may actually contain IL-22 that could react with the assay.

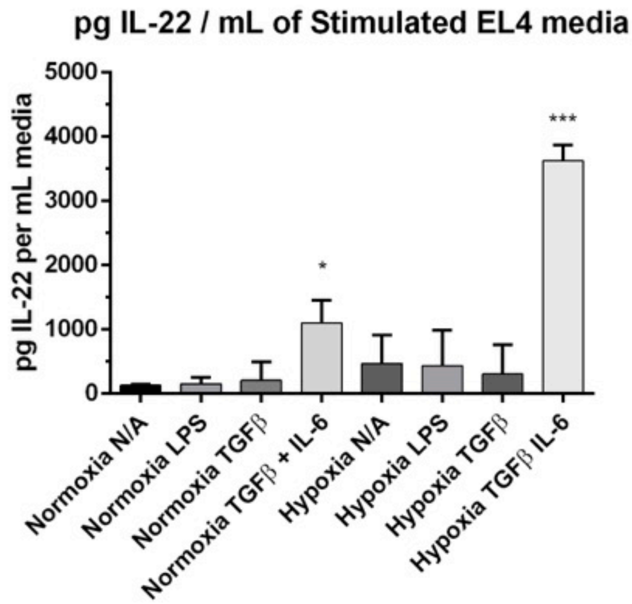

Figure 34: IL-22 Production by Stimulated EL4 Cells. Assayed by ELISA (error bars indicate standard deviation, n = 2, * $p < .05$, *** $p < .001$ by one-way ANOVA with post-hoc Dunnett's test for multiple comparisons)

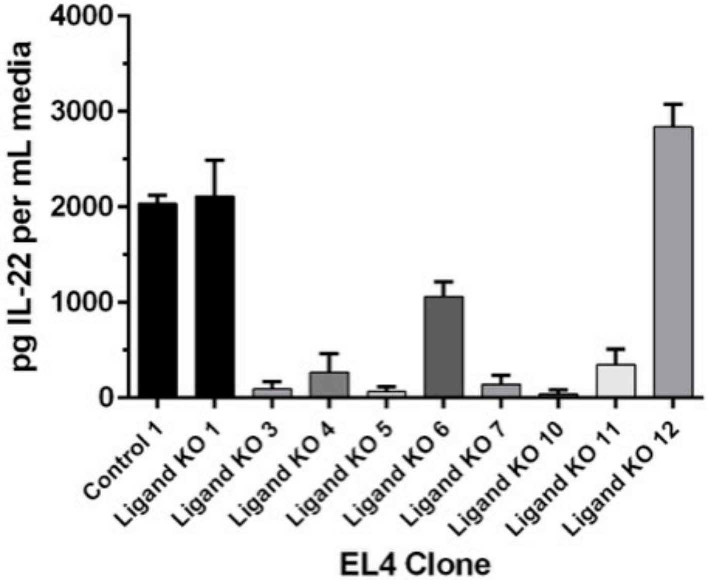

Figure 35: IL-22 Production by Stimulated EL4 Cells Following CRISPR Targeted IL-22 Ligand Knockout. Assayed by ELISA. (error bars indicate standard deviation, n = 4 technical replicates for each clone assayed).

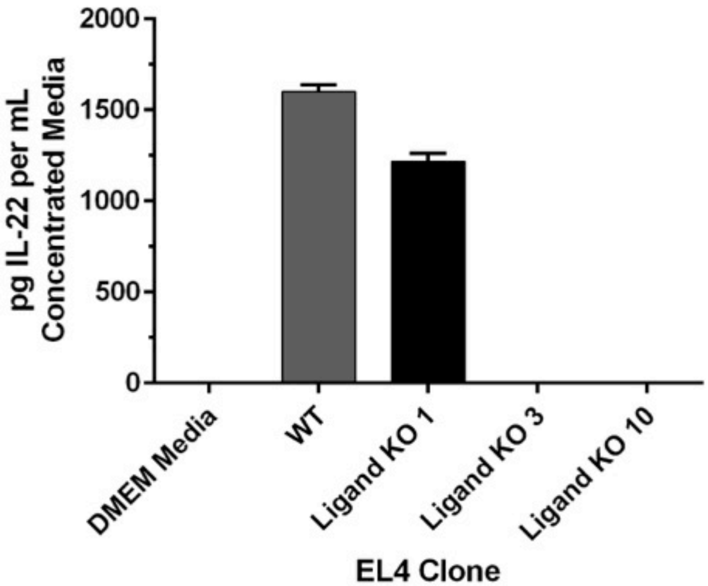

Figure 36: IL-22 Levels in Concentrated Media Collected from Stimulated CRISPR Knockout EL4 Clones. Assayed by ELISA. (error bars indicate standard deviation, n = 4 technical replicates for each clone assayed)

3.2.5 - Effects of CRISPR-Cas 9 IL-22 ligand knockout *in-vivo*

The aforementioned clones 3 and 10 were injected in nude mice, and found to result in a statistically significant decrease in tumor growth compared to a control KO clone, named control 1, as well as compared to WT cells (Figure 37). An ELISA assay for IL-22 within the homogenized tumors found no detectable levels of IL-22 from the mouse tumors derived from both clones 3 and 10 (Figure 38). This suggests that in athymic nude mice, any IL-22 in the tumors is derived from the EL4 cells themselves, and not from infiltrating immune cells.

Since the control 1 clone actually grew most quickly in the nude mice, the decision was made to switch to another ligand knockout clone as a control. Ligand knockout clone 6 was chosen, as it had undergone the CRISPR-Cas9 transfection procedure and sorting, but was found on ELISA to actually produce detectable levels of IL-22. This clone, alone with clones 3, 10, and wild type EL4 cells were injected in athymic nude mice and treated with either anti-VEGF antibody or isotype control antibody. In the animals treated with IgG2A isotype control, the clone subtype had no statistically significant effect on tumor growth (Figure 39). In those treated with anti-VEGF antibody, however, clones 6 and 10 had a statistically significant reduction in tumor growth (Figure 40). While clone 3 had produced a statistically significant decrease in tumor growth compared to wild type in the untreated animals, it failed to repeat the same effect in this experiment. As such, it appears that despite all of the clones being derived from the same batch of wild-type cells, there is inherent variability in their cell growth *in-vivo*.

ELISA assays for IL-22, IL-17, and VEGF were conducted on mice from both IgG2A and anti-VEGF treatment groups (Figures 41-49). As previously observed, clones 3 and 10 in both treatment groups lacked detectable levels of IL-22 (Figure 41). Interestingly, clone 10 had statistically elevated levels of IL-17 production (Figure 42). Of note, clone 10 produced the smallest tumors at endpoint in both nude mice studies conducted with CRISPR knockout EL4 clones. While a previous study had shown that IL-17 can mediate resistance to VEGF, when examining IL-17 levels in both isotype treated animals (Figure 48) and those treated with anti-VEGF (Figure 49), the IL-17 levels in both groups were significantly higher in tumors derived from clone 10. The mice treated with anti-VEGF therapy had higher levels of IL-17 regardless of the clone used, although the levels of clone 10 were greater, relatively, among this treatment group.

Among EL4 clones in both treatment groups, there was no difference in VEGF levels (Figure 43). The animals treated with anti-VEGF therapy, however, had higher levels of VEGF within their tumors compared to those treated with isotype control antibody (Figures 46-47). As previous studies have suggested, this is could be due either to sequestration of VEGF within the tumors by the antibody, or biological upregulation of VEGF production either by the tumor cells themselves or the stroma[81].

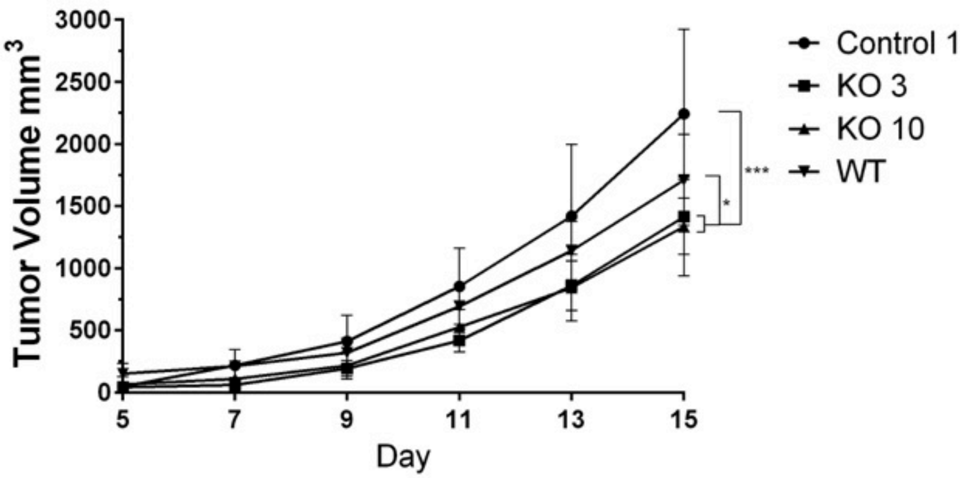

Figure 37: EL4 Tumor Growth in Athymic Nude Mice. (error bars indicate standard deviation, n = 5, * p < .05, *** p < .001 by two way ANOVA with post-hoc Tukey's test for multiple comparisons)

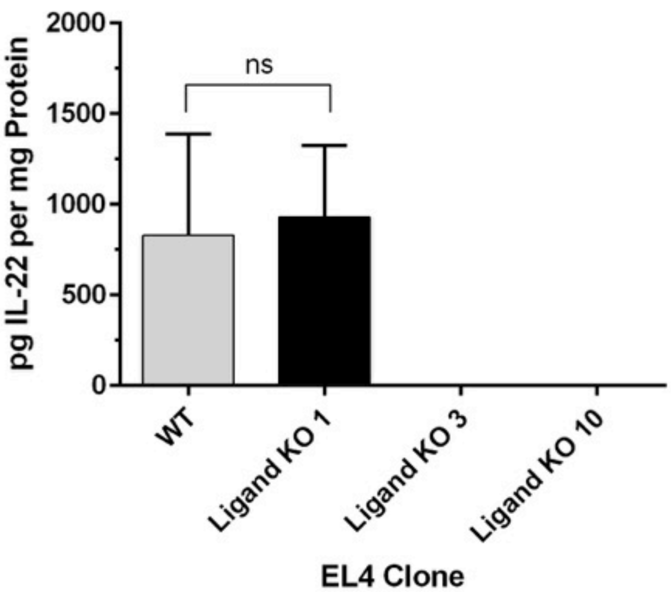

Figure 38: Tumor IL-22 Levels in EL4 CRISPR Clone Bearing Athymic Nude Mice. Assayed by ELISA. (error bars indicate standard deviation, n = 5, ns = not significant by one-way ANOVA with post-hoc Tukey's test for multiple comparisons)

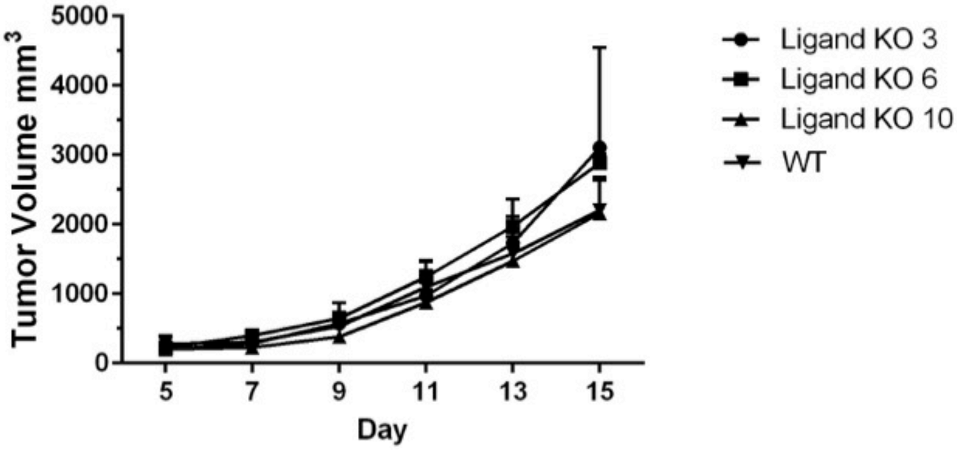

Figure 39: EL4 CRISPR Clone Growth in Athymic Nude Mice Treated with IgG2A Isotype Antibody. (error bars indicate standard deviation, n = 5, ns = not significant by two-way ANOVA with post-hoc Tukey's test for multiple comparisons)

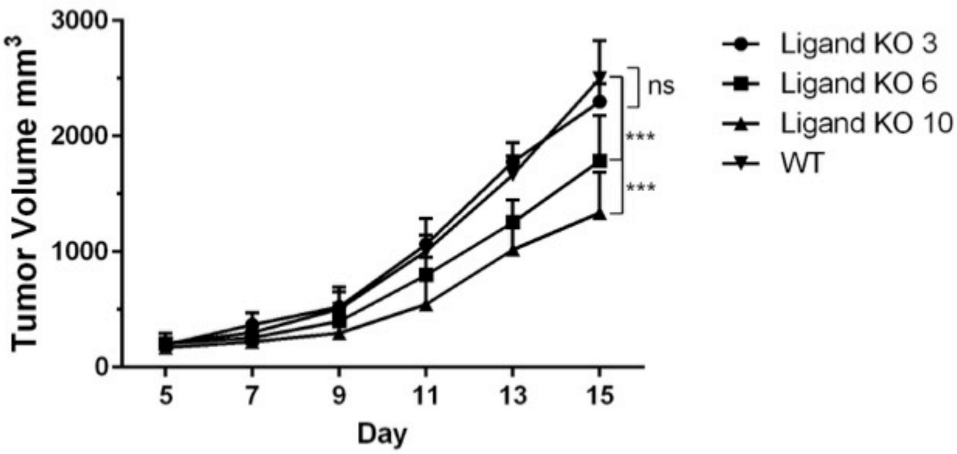

Figure 40: Mouse EL4 CRISPR Clone Growth in Athymic Nude Mice Treated with Anti-VEGF Antibody. (error bars indicate standard deviation, $n = 5$, ns = not significant, *** $p < .001$ by two-way ANOVA with post-hoc Tukey's test for multiple comparisons)

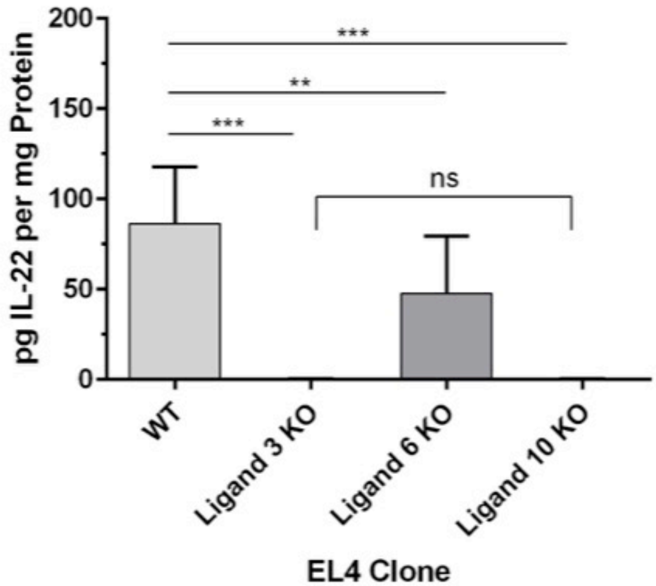

Figure 41: Tumor IL-22 Levels in EL4 CRISPR Clone Bearing Athymic Nude Mice. Assayed by ELISA. (error bars indicate standard deviation, n = 10, ns = not significant, ** p < .01, *** p < .001 by one-way ANOVA with post-hoc Tukey's test for multiple comparisons)

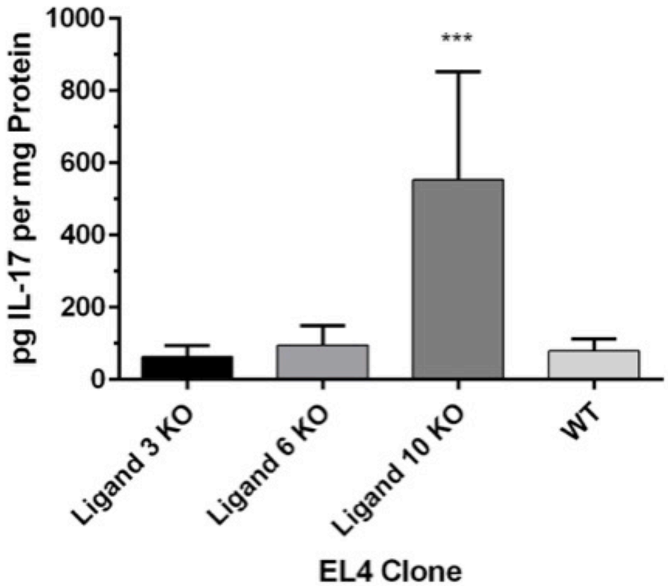

Figure 42: Tumor IL-17 Levels in EL4 CRISPR Clone Bearing Athymic Nude Mice. Assayed by ELISA. (error bars indicate standard deviation, n = 10, *** p < .001 by one-way ANOVA with post-hoc Tukey's test for multiple comparisons)

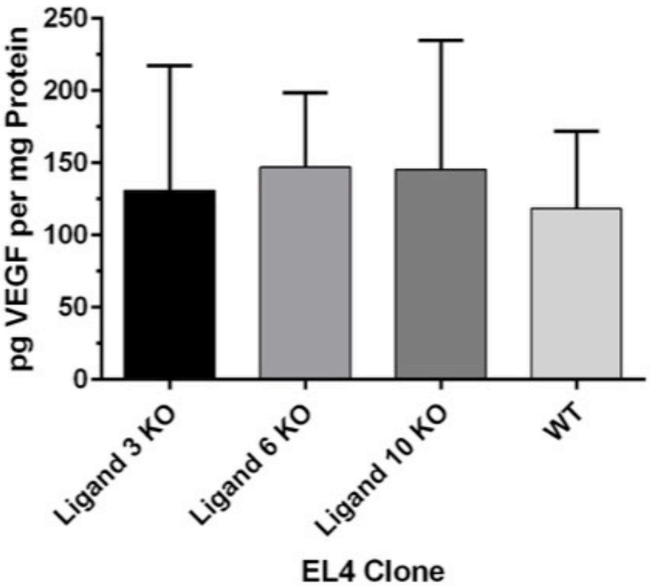

Figure 43: Tumor VEGF Levels in EL4 CRISPR Clone Bearing Athymic Nude Mice. Assayed by ELISA. (error bars indicate standard deviation, n = 10, ns = not significant by one-way ANOVA with Tukey's test for multiple comparisons)

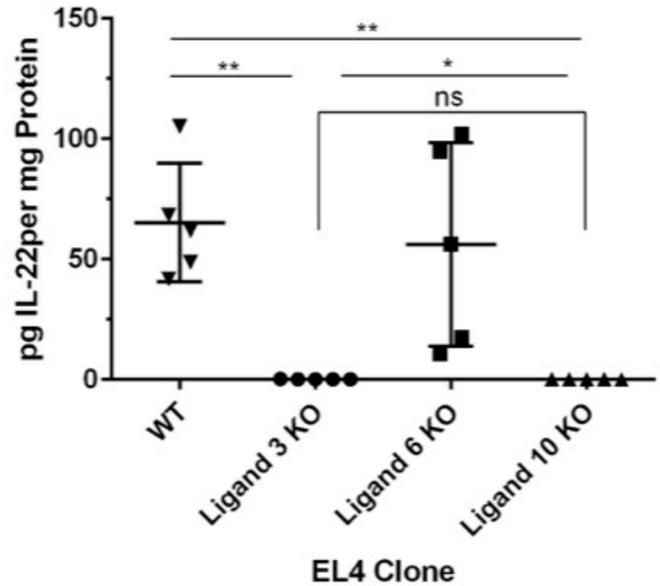

Figure 44: Tumor IL-22 Levels in EL4 CRISPR Clone Bearing Athymic Nude Mice Treated with IgG2A Isotype Antibody. Assayed by ELISA. (error bars indicate standard deviation, n = 5, ns = not significant, * p < .05, ** p < .01 by one-way ANOVA with post-hoc Tukey's test for multiple comparisons)

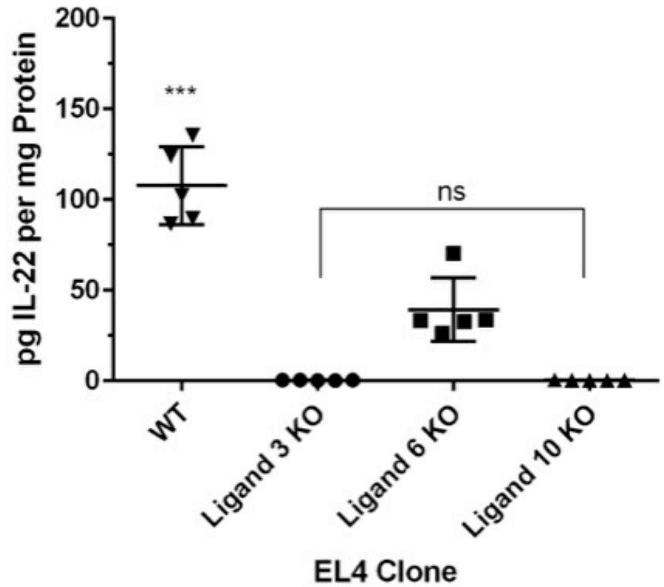

Figure 45: Tumor IL-22 Levels in EL4 CRISPR Clone Bearing Athymic Nude Mice Treated with Anti-VEGF Antibody. Assayed by ELISA. (error bars indicate standard deviation, n = 5, ns = not significant, *** p < .001 by one-way ANOVA with post-hoc Tukey's test for multiple comparisons)

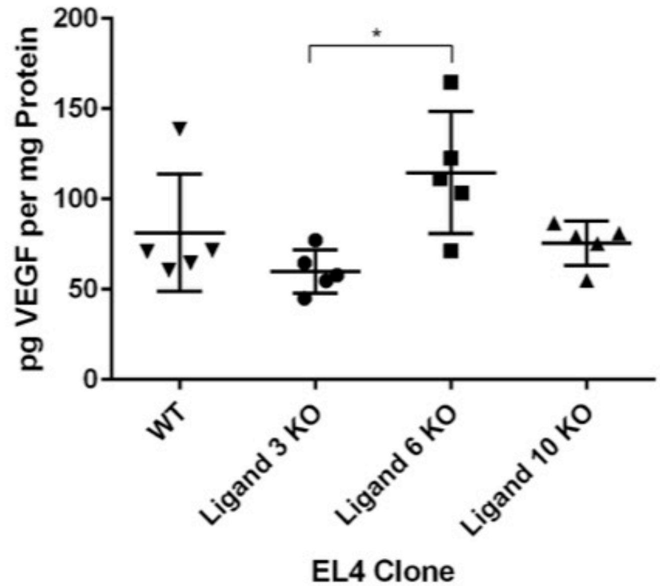

Figure 46: Tumor VEGF Levels in EL4 CRISPR Clone Bearing Athymic Nude Mice Treated with IgG2A Isotype Antibody. Assayed by ELISA. (error bars indicate standard deviation, n = 5, * $p < .05$ by one-way ANOVA with post-hoc Tukey's test for multiple comparisons)

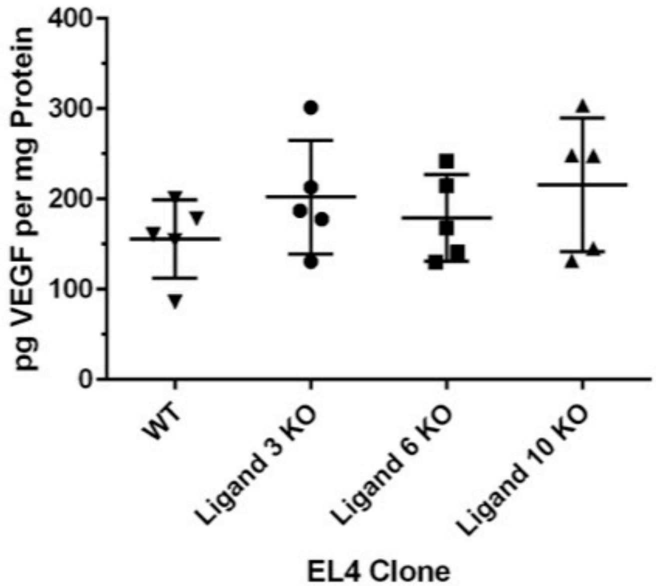

Figure 47: Tumor VEGF Levels in EL4 CRISPR Clone Bearing Athymic Nude Mice Treated with Anti-VEGF Antibody. Assayed by ELISA. (error bars indicate standard deviation, n = 5, ns = not significant by one-way ANOVA with post-hoc Tukey's test for multiple comparisons)

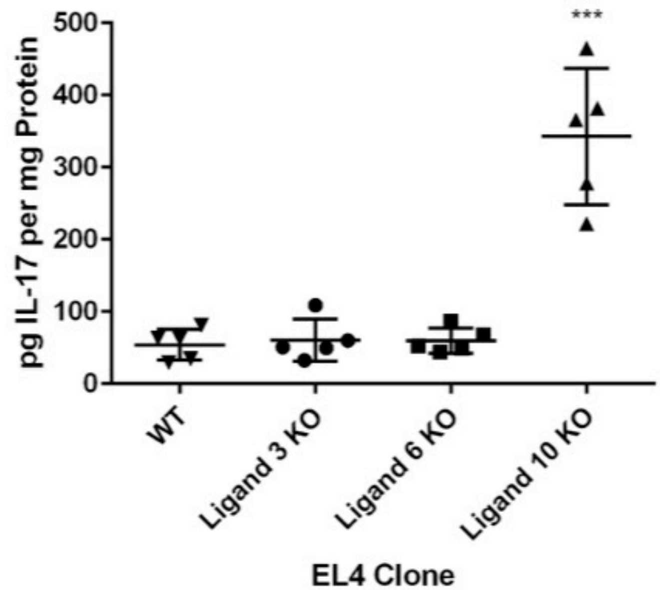

Figure 48: Tumor IL-17 Levels in EL4 CRISPR Clone Bearing Athymic Nude Mice Treated with IgG2A Isotype Antibody. Assayed by ELISA. (error bars indicate standard deviation, n = 5, ns = not significant, *** p < .001 by one-way ANOVA with post-hoc Tukey's test for multiple comparisons)

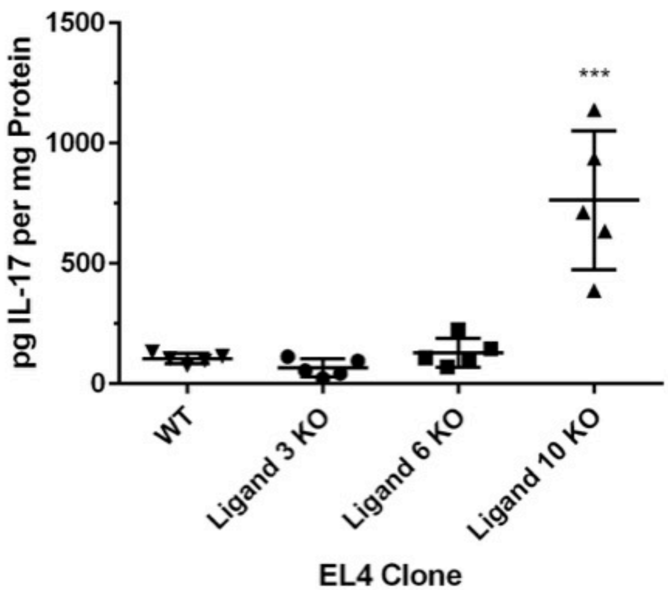

Figure 49: Tumor IL-17 Levels in EL4 CRISPR Clone Bearing Athymic Nude Mice Treated with Anti-VEGF Antibody. Assayed by ELISA. (error bars indicate standard deviation, n = 5, ns = not significant, *** p < .001 by one-way ANOVA with post-hoc Tukey's test for multiple comparisons)

3.3 - Discussion

This investigation yielded several important findings. First, it was confirmed that EL4 cells can produce detectable levels of interleukin-22 *in-vitro*, and that higher levels are produced in the setting of hypoxia than normoxia. Tumors are known to have decreased oxygen saturation, which is a major mechanism by which they can induce angiogenesis. The observation that decreased oxygen levels also increase IL-22 production appears consistent with the potential for IL-22 to mediate tumor growth through a paracrine network in an EL4 model. It was also confirmed that neither IL-22 addition nor blockade affected the growth of EL4 cells *in-vitro*. Blocking IL-22 reduced tumor growth in “wild type” C57BL/6 mice, immunodeficient athymic nude mice lacking functional CD4+ T-cells, as well as in Rag1$^{-/-}$ mice lacking any functional adaptive immune cells. Interestingly, the C57BL/6 mice had the lowest tumor levels of IL-22, despite having the most active immune system of the three mouse models investigated. A CRISPR-Cas9 knockout was ultimately not able to provide conclusive evidence that EL4 cells that lack IL-22 production would grow more slowly than wild-type EL4 cells *in-vivo*. It was found, however, that the tumors isolated from athymic nude mice bearing EL4 clones that did not produce any IL-22 *in-vitro* also lacked detectable levels of IL-22 by ELISA. This strongly suggests the IL-22 measured within EL4 tumors is derived from the EL4 cells themselves, and not from infiltrating lymphocytes or monocytes. While more work is needed to elucidate the particular paracrine mechanisms by which inhibiting IL-22 can reduce tumor growth, it is evident across multiple murine models that IL-22 blockade can consistently inhibit tumor growth *in-vivo*.

Chapter 3, in part, is currently being prepared for submission for publication of the material. Protopsaltis, N.; Liang, W.; Nudleman, E.; Ferrara, N. The dissertation author was the primary investigator and author of this material.

CHAPTER 4.

Effects of IL-22 in a GL261 Tumor Model

4.1 - Introduction

Use of an EL4 model demonstrated that blocking IL-22 can reduce tumor growth *in-vivo*. While EL4 cells produce IL-22 *in-vitro* and *in-vivo*, the glioblastoma tumor model GL261 was chosen as an additional model for its predicted lack of endogenous IL-22 production, and was postulated to lack IL-22 receptor expression based on tissue-specific expression studies[45]. Glioblastomas are highly vascularized, and as a result, glioblastoma multiforme is one of the cancers for which the anti-VEGF antibody bevacizumab has been FDA approved. This chapter examines the role of IL-22 on GL261 tumor cells both *in-vitro* and *in-vivo*.

4.2 - Results

4.2.1 - GL261 does not express IL-22 receptor

Simultaneous investigation of GL261 along EL4 demonstrated that GL261 cells do not express the IL-22Rα1 subunit (Figure 21). It was important to show that GL261 cells lack this receptor, as GL261 expression of the IL-22R could affect cell growth with either addition or blockade of IL-22 *in-vitro*.

4.2.2 - Neither addition nor blockade of IL-22 affects GL261 growth in-vitro

To examine the effects of IL-22 in tumor angiogenesis, it was first necessary to ensure that IL-22 did not have a direct effect on GL261 cells themselves. Adding IL-22 to GL261 cells in culture did not result in an increase in cell number after 6 days, determined by an alamar blue cell viability assay (Figure 50). Doses from 5 to 100 ng IL-22 / mL failed to increase cellular proliferation compared to PBS control, whereas cells plated in the presence of 10% FBS resulted in a cell number approximately 3 fold greater at endpoint compared to PBS control.

The use of GL261 as a model system to investigate the role of IL-22 in tumor growth and angiogenesis ultimately requires administration of an anti-IL22 antibody. Although IL-22 did not increase GL261 proliferation *in-vitro*, it was necessary to ensure that IL-22 antibody blockade would not directly inhibit

GL261 cell growth, as this could confound the effects of the antibody blockade on GL261 tumor growth *in-vivo*. Increasing doses of anti-IL-22 antibody did not result in decreased cell growth compared to IgG1A antibody treatment after 6 day incubation (Figure 51). Not only was there no decrease in cell growth between anti-IL22 antibody and IgG1A control, but there was no effect of antibody dose from 0.5 to 50 μg / mL for either antibody added *in-vitro*. Anti-VEGF antibody serves as a control and comparison for *in-vivo* studies, and was also investigated for its ability to inhibit GL261 growth *in-vitro*. 50 μg / mL of anti-VEGF antibody did not inhibit GL261 growth compared to media alone (Figure 52). In summation, the data observed indicates that neither IL-22 addition nor blockade has a direct effect on GL261 cells growth *in-vitro*.

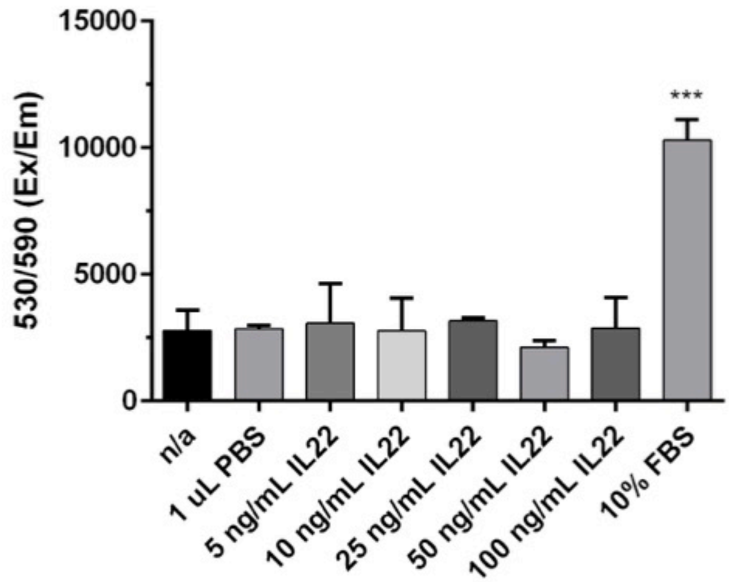

Figure 50: IL-22 Does Not Promote GL261 Proliferation. Assessed by alamar blue viability assay. (error bars indicate standard deviation, n = 2, *** $p < .001$ by one-way ANOVA with post-hoc Dunnett's test for multiple comparisons)

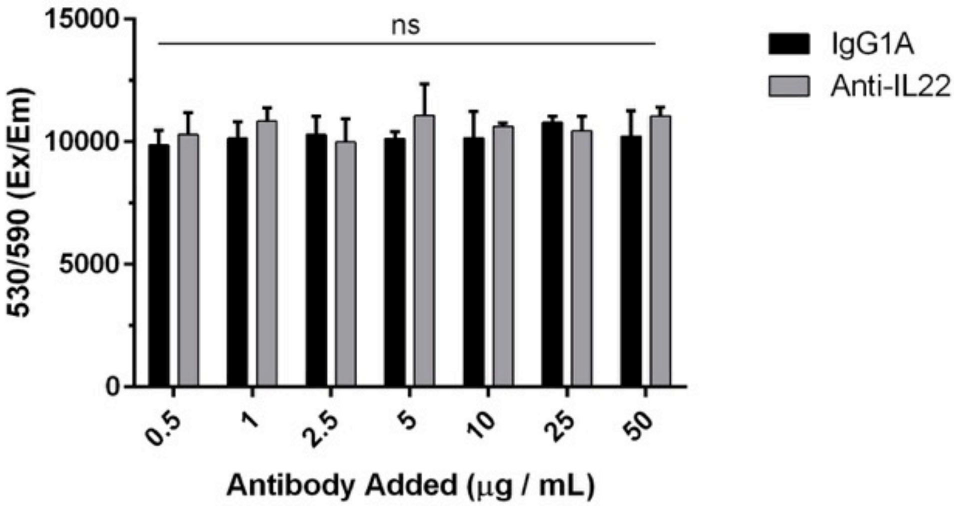

Figure 51: Anti-IL22 Antibody Does not Inhibit GL261 Growth in Vitro. Assessed by alamar blue viability assay. (error bars indicate standard deviation, n = 3, ns = not significant by two-way ANOVA with post-hoc Šidák's correction for multiple comparisons)

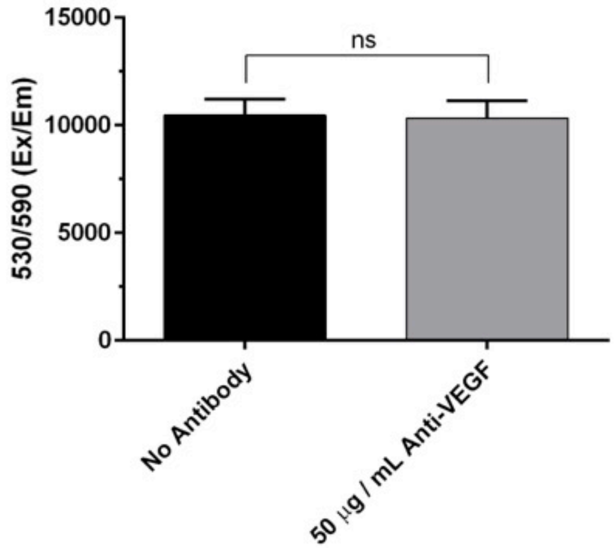

Figure 52: Anti-VEGF Antibody Does not Inhibit GL261 Growth in Vitro. Assessed by alamar blue viability assay. (error bars indicate standard deviation, n = 6, ns = not significant by Welch's unpaired t-test)

4.2.3 - GL261 cells do not produce IL-22 *in-vitro*

While EL4 was chosen for its ability to produce IL-22, it was postulated that as a glioblastoma, it was unlikely GL261 cells would produce IL-22. Indeed, GL261 conditioned media did not contain detectable levels of IL-22 by ELISA (Figure 53). As a control, recombinant murine IL-22 was added, along with the anti-IL22 antibody. IL-22 addition alone demonstrated readout levels beyond the functional range of the ELISA assay, but addition of anti-IL22 antibody reduced the detected levels. Antibody was also added to the DMEM media alone, as well as to the GL261 conditioned media, neither of which demonstrated detectable IL-22 levels in the ELISA assay. Not only did these controls reveal that the anti-IL22 antibody can sequester and reduce detectable IL-22 in the ELISA assay, but that the antibody in and of itself can not react with the ELISA assay to give false-positive results.

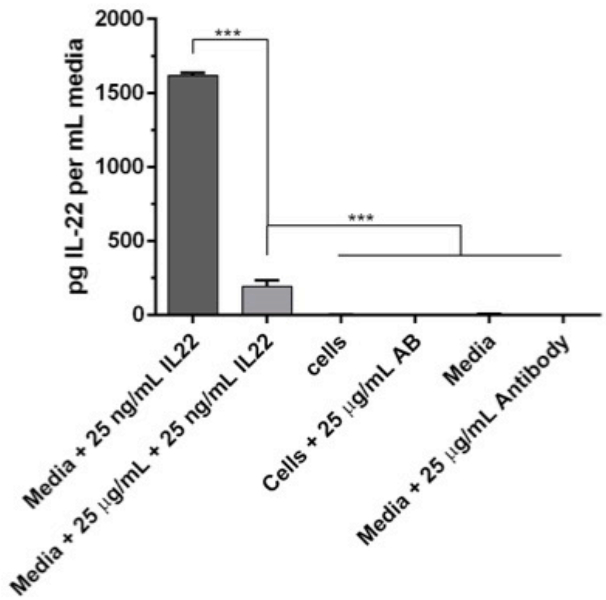

Figure 53: IL-22 Levels in GL261 Tumor Conditioned Media. (error bars indicate standard deviation, n = 2 technical replicates, *** p < .001 by one-way ANOVA with post-hoc Tukey's test for multiple comparisons)

4.2.4 - Blocking IL-22 reduces GL261 tumor growth in-vivo

After ensuring that the blockade of IL-22 would not directly inhibit the growth of GL261 cells, they were injected into the flanks of C57BL/6 mice. Administration of anti-VEGF antibody resulted in a statistically significant decrease in tumor growth compared to IgG1A isotype control antibody treatment (Figure 54). Anti-IL22 antibody treatment also resulted in a significant decrease compared to isotype control, and the effect was statistically equivalent to the anti-VEGF therapy. ELISA analysis revealed an increase of intra-tumor IL-22 in the mice treated with anti-VEGF but not anti-IL22 antibody (Figure 55). Interestingly, despite not producing detectable levels of IL-22 in-vitro, it appears that GL261 tumors contain IL-22 in-vivo.

Given the effects of IL-22 on endothelial cells, it was conceivable that IL-22 and VEGF could be acting synergistically to enhance tumor growth. Although studies in EL4 tumor bearing mice failed to demonstrate a greater reduction for combination antibody treatment than either therapy alone, to address this possibility with a GL261 model, anti-IL22 and anti-VEGF combination therapy were given to GL261 tumor bearing athymic nude mice (Figure 56). Having observed intra-tumor IL-22 in the GL261 tumors from C57BL/6 mice, nude mice were chosen as an attempt to eliminate T-cell sources of IL-22 and ascertain if the IL-22 was indeed derived from the glioblastoma tumors themselves. Both anti-IL22 and anti-VEGF monotherapy resulted in a significant reduction in tumor growth compared to isotype control treatment. While Combination anti-IL22 and anti-VEGF treatment resulted in the greatest reduction in tumor growth compared to isotype control, the combination therapy did not result in a statistically significant difference compared to either therapy alone. Of note, this was the same effect that was observed in an EL4 tumor model.

ELISA analysis on these tumors revealed that the mice treated with anti-VEGF monotherapy, but not anti-IL22 treatment, had higher levels of IL-22 compared to those treated with isotype control antibody (Figure 57). Those treated with combination anti-IL22 and anti-VEGF therapy had the highest levels of intratumor IL-22.

CD31b staining on GL261 tumors from C57BL/6 mice revealed no difference in the percent area that was positively stained (Figure 58).

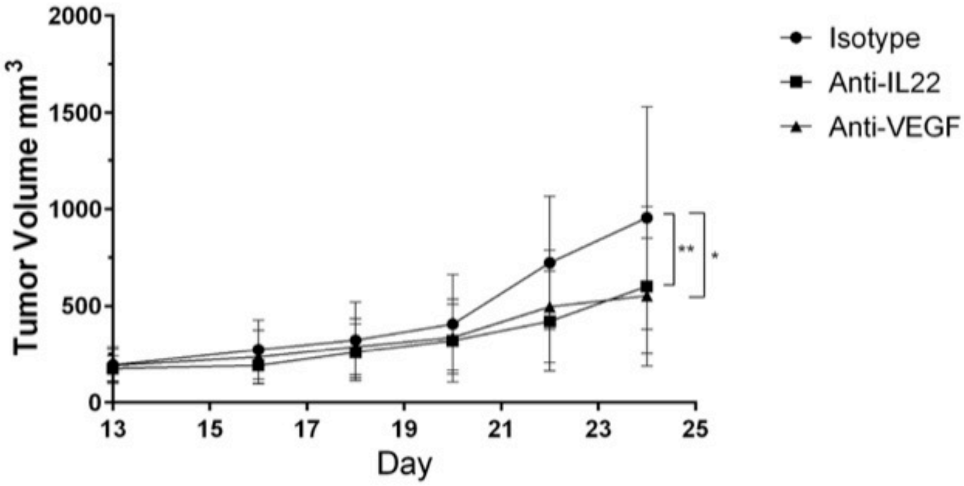

Figure 54: Anti-IL22 Antibody Treatment Reduces GL261 Tumor Growth in C57BL/6 Mice. (error bars indicate standard deviation, n = 9 - 10, * p < .05, ** p < .01 by two-way ANOVA with post-hoc Tukey's test for multiple comparisons)

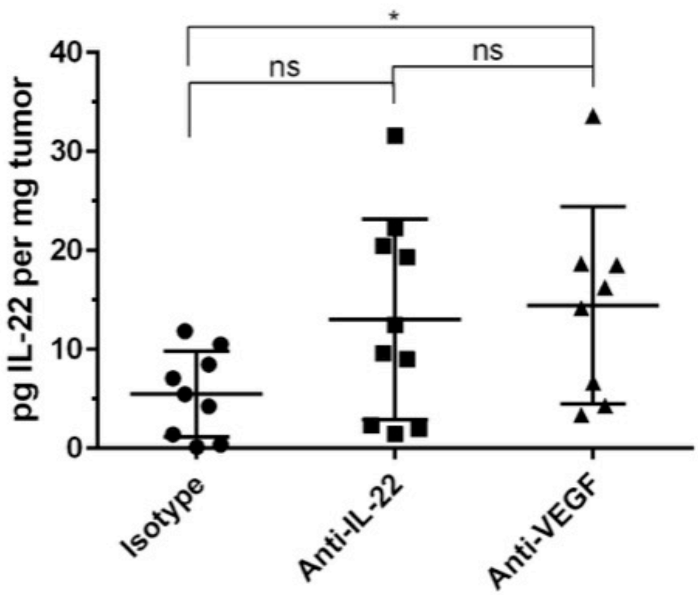

Figure 55: GL261 Tumor IL-22 Levels in C57BL/6 Mice. Assessed by ELISA. (error bars indicate standard deviation, n = 8 - 10, ns = not significant, * $p < .05$ by Welch's unpaired t-test)

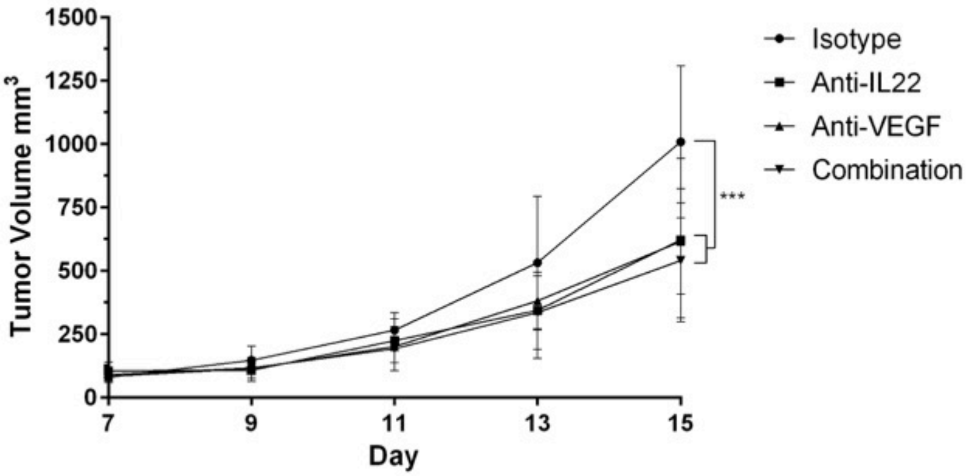

Figure 56: Anti-IL22 Antibody Treatment Reduces GL261 Tumor Growth in Athymic Nude Mice. (error bars indicate standard deviation, n = 10, *** $p < .001$ by two-way ANOVA with post-hoc Tukey's test for multiple comparisons)

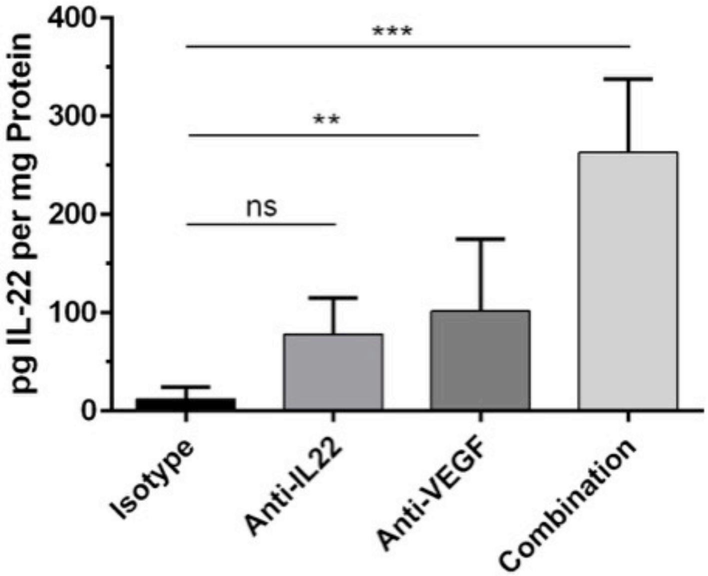

Figure 57: GL261 Tumor IL-22 Levels in Athymic Nude Mice. Assessed by ELISA. (error bars indicate standard deviation, n = 10, ns = not significant, ** p < .01, *** p < .001 by one-way ANOVA with post-hoc Tukey's test for multiple comparisons)

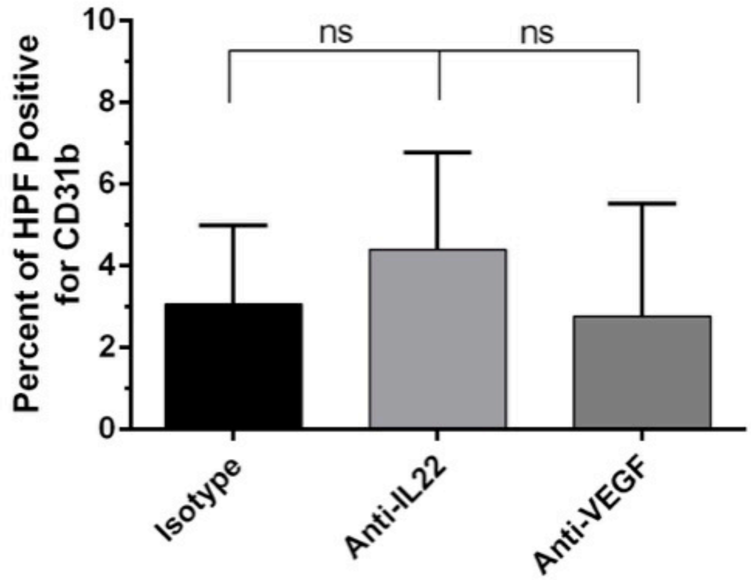

Figure 58: Neither Anti-IL22 nor Anti-VEGF Antibody Treatment Reduces The Percent Area Stained for CD31b in GL261 Tumors From C57BL/6 Mice. (error bars indicate standard deviation, n = 2-5, ns = not significant by one-way ANOVA with post-hoc Dunnett's test for multiple comparisons)

4.3 - Discussion

It was found that IL-22 does not directly stimulate GL261 cell growth *in-vitro,* which contrasts a report published during the process of this study[82]. While the researchers measured IL-22 binding protein in mouse tumors, the data does not indicate that they directly examined IL-22R. Having demonstrated that GL261 cells lack IL-22 receptor expression, it seems unlikely that IL-22 could directly stimulate GL261 growth *in-vitro*, which is in accordance with the data reported here. The same researchers found that IL-22 can promote GL261 growth *in-vivo* through combination of IL-22 knockout and directly injecting IL-22 into the brains of mice with GL261 tumors. While GL261 was studied subcutaneously in this work, it was found that the tumors endogenously contained detectable levels of IL-22, despite the observation that IL-22 was undetectable by ELISA *in-vitro*. During initial characterization of IL-22, it was observed that murine spleen cells did not produce IL-22 when stimulated *in-vitro*, yet demonstrated IL-22 production *in-vivo*[42]. The investigators postulated that this discrepancy could arise from differential or indirect mechanisms of IL-22 induction, and hence it is possible that the same effects are true regarding GL261 production of IL-22 *in-vivo,* and lack thereof *in-vitro*.

It was found that IL-22 levels in mice treated with anti-VEGF therapy were significantly higher than those treated with isotype antibody. This suggests that IL-22 may be upregulated in GL261 tumors *in-vivo* as a method of escaping anti-angiogenic pharmacological inhibition. Despite the tumor inhibition observed *in-vivo* following anti-IL22 and anti-VEGF therapy, staining for CD31b did not demonstrate a statistically significant difference in blood vessel density for treated GL261 tumor bearing mice.

The anti-angiogenic effect of a therapy, however, is more complicated than simply the density of blood vessels within the tumor[83]. Some studies have shown that angiogenesis inhibitors can actually increase tumor blood flow and oxygenation during the initial few weeks of treatment, and furthermore, that some benefit of anti-angiogenic therapy may arise from reducing interstitial pressure[84,85,13]. Additionally, while it is well accepted that VEGF can promote tumor growth and neovascularization, paradoxically, pharmacologic inhibitors do not always allow for understanding the contribution of VEGF to angiogenesis[86,87].

In the setting of GL261 bearing mice, anti-IL22 and anti-VEGF therapy both resulted in a statistically significant decrease in tumor growth, but not blood vessel density. It is possible that they may slow down the initial process of angiogenesis, i.e. vessel sprouting, but as the tumor secretes increasing quantities of IL-22, among other growth factors, the pharmacologic inhibition fails to suppress new vessel formation. As such, perhaps immunofluorescence staining at an earlier time point during tumor growth would reveal that the treatment does in fact reduce tumor blood vessel density. Given that anti-VEGF therapy is well-known to reduce angiogenesis, it could be argued that the lack of significant difference observed in treated GL261 bearing mice suggests that staining for microvessel density in GL261 tumors at the end point chosen is not indicative for the ability of a treatment to reduce to angiogenesis. In other words, the lack of reduction in CD31b staining in GL261 bearing mice treated with anti-IL22 antibody does not necessarily mean that blocking IL-22 cannot reduce tumor angiogenesis. This is especially plausible given the results observed on endothelial cells in-vitro, the reduction in tumor growth by anti-IL22 treatment in both an EL4 and GL261 model, and the reduction in vessel density observed in the EL4 model.

Furthermore, the GL261 tumors demonstrated significant necrosis and fluid accumulation. Staining for CD31b is contingent on having solid tumor with enough cross sectional area for quantification. It is possible that the anti-VEGF and anti-IL22 treatment reduced tumor growth, but that there was consistent vessel density along the tumor periphery, i.e. non-necrotic portion. As such, there may be systemic error inherent from needing to measure vessel density in portions of tumor amenable to staining, even if the treatments did in fact reduce neovascularization resulting in tumor hypoxia, necrosis, and reduction of growth. Further studies using *in-vivo* live imaging of vessel parameters are a potentially worthwhile future endeavor that would bypass this limitation, and would provide valuable insight to the effects of anti-angiogenic therapy.

In summation, IL-22 blockade results in a reduction of GL261 growth in-vivo. These findings, taken in combination with the effects observed on endothelial cells by IL-22, suggests that IL-22 may promote angiogenesis in glioblastoma, although further work is needed to definitively elucidate the mechanisms observed.

Chapter 4, in part, is currently being prepared for submission for publication of the material. Protopsaltis, N.; Liang, W.; Nudleman, E.; Ferrara, N. The dissertation author was the primary investigator and author of this material.

CHAPTER 5.

Materials and Methods

Materials

Mice

Female (6-8 week) C57BL/6 and Rag1-/- mice were purchased from Jackson Laboratories and were allowed 5 days to acclimate following arrival. Female (6-8 week) athymic nude mice were purchased from the University of California, San Diego. Animals were housed in clean cages and experimental procedures were carried out under pathogen-free conditions in accordance with established standards of care and approved protocols from the Animal Care and Use Committee of the University of California, San Diego. Prior to tissue harvest, mice were euthanized by CO_2 inhalation followed by cervical dislocation.

Cells

Primary human umbilical vein endothelial cells (HUVEC, passage 4–8) were purchased from Lonza and cultured on 0.1% gelatin-coated plates in EGM-2 endothelial cell growth media. Primary human lung microvascular endothelial cells (MVEC, passage 3-6) were purchased from Lonza and cultured on 0.1% gelatin coated plates in EGM-2 microvascular cell growth media. EL4 cells were purchased from ATCC and maintained in high glucose Dulbecco's modified Eagle's medium (DMEM) supplemented with 10% fetal bovine serum (FBS). GL261 cells were a gift from Dr. Santosh Kesari and maintained in high glucose Dulbecco's modified Eagle's medium (DMEM) supplemented with 10% fetal bovine serum (FBS). Cells were maintained at 37°C in a humidified atmosphere with 5% CO_2.

Reagents

Alamar Blue	Fisher Scientific	Cat#PI88952
Crystal Violet Solution	Sigma-Aldrich	Cat#HT90132-1L
P-ErK 1/2	Cell Signaling Tech. Inc.	Cat#4376S
Erk 1/2	Cell Signaling Tech. Inc.	Cat#4695S
Anti-VEGF mAb B20.4.1	Genentech	N/A
Mouse IgG1A	Bio X Cell	Cat#BE0083
Mouse IgG2A	Bio X Cell	Cat#BE0085
Trypsin	Thermo Fisher Scientific	Cat#90057
NuPAGE® LDS Sample Buffer (4x)	Fisher Scientific	Cat#NP0007
Human $VEGF_{165}$	R&D Systems	Cat#293-VE
Human bFGF	PeproTech	Cat#100-18B

Cultrex Reduced Growth Factor Basement Membrane Extract	Trevigen	Cat#3433-005-R1
DMEM (high glucose)	Hyclone	Cat#SH30243.01
DMEM (low glucose)	Hyclone	Cat#SH30021.01
FBS	Omega Scientific	Cat#FB-02
Lipofectamine 3000 Transfection Reagent	Life Technologies	Cat#L3000075
EBM-2	Lonza	Cat#CC3156
EGM-2	Lonza	Cat#CC3162
EGM-2MV	Lonza	Cat#CC3202
Murine IL-22	Cell Signaling	Cat#5224SF
Human IL-22	Cell Signaling	Cat#8931SF
PAGE gels	Life Technologies	Cat# NP0336BOX
Mouse IL-22 ELISA	R&D Systems	Cat#M2200
Mouse IL-17 ELISA	R&D Systems	Cat#M1700
Mouse VEGF ELISA	R&D Systems	Cat#MMV00
Anti-IL-22Rα1	Invitrogen	Cat#PIPA130723
Anti- Mouse IL22Rα1 PE	R&D Systems	Cat#FAB42941P
Anti-Human IL22Rα1 PE	R&D Systems	Cat# FAB2770P
Mouse IgG1A PE	R&D Systems	Cat# IC002P
Anti-IL22 mAb 8E11	Genentech	N/A
Rat IgG2A PE	R&D Systems	Cat# IC006P

Anti-P-AKT	Cell Signaling	Cat# 4060S
Anti-AKT	Cell Signaling	Cat# 4691S
Anti-P-STAT3	Cell Signaling	Cat# 9145S
Anti-STAT3	Cell Signaling	Cat# 4904S
Anti-B-Actin	Sigma Aldrich	Cat#A2228
CRISPR Plasmid IL-22	Santa Cruz Biotechnology	Cat#SC-424538
CRISPR Plasmid Control	Santa Cruz Biotechnology	Cat#SC-418922
Nucleofector kit L	Lonza	Cat#VACA-1005
Anti-mouse CD31b	BD Biosciences	Cat#550274
Murine IL-6	Peprotech	Cat#216-16
Anti-IL22Rα1 siRNA	Thermo Fisher	Cat#1299001
Control siRNA	Thermo Fisher	Cat#4390843
Cell Lysis buffer 2	R&D Systems	Cat#895347
ProLong Gold Mountant	Life Technologies	Cat#P36930
Propidium Iodide	Biolegend	Cat#421301

Method Details

Conditioned Media Preparation and IL-22 ELISA

One million EL4 cells in 25 cm^2-flasks were stimulated with cytokines as noted. Cells were grown in a 37°C humidified atmosphere with ambient O_2 in the setting of normoxia, or a 37°C humidified atmosphere with 1% O_2 in the setting of hypoxia. After 6 days, media were collected. IL-22 concentrations were measured using a murine R&D systems IL-22 Quantikine ELISA kit according to the manufacturer's instructions.

Western Blots

HUVECs between passages 6 and 8 were seeded onto 6 or 12-well dishes pretreated with a 1% gelatin solution. The cells were starved overnight in EBM-2 solution supplemented with 2% FBS. The next morning, cells were rinsed with EBM-2 media, and starved in EBM-2 media containing 0.1% FBS for 4 hours. The media was then refreshed again containing cytokines of interest and stimulated for the time indicated. The cells were then rinsed with ice-cold PBS, lysed with RIPA buffer supplemented with 1% phosphatase/protease inhibitor, and collected with a cell scraper. The lysate was placed on a rotating inverter for 10 minutes, centrifuged for 30 minutes at 14000 x g, and the supernatant collected by pipette. Lysates were diluted with 4X running buffer and 10% β-Mercaptoethanol, heated for at least 5 minutes at 95°C, and run by SDS-PAGE. Protein was transferred to nitrocellulose membranes for antibody staining and quantification as indicated.

Endothelial Cell Proliferation Assays

HUVECs between passages 6 and 8 were seeded onto 12-well dishes pretreated with a 0.1% gelatin solution. The cells were starved overnight in EBM-2 solution supplemented with 2% FBS. The next morning, cells were rinsed with EBM-2 media, and refreshed with EBM-2 solution supplemented with 10% FBS containing cytokines of interest and incubated for 3 days.

MVECs between passages 3 and 6 were starved overnight in EBM-2 solution supplemented with 2% FBS. The next morning, cells were rinsed with EBM-2 media and seeded with EBM-2 solution supplemented with 2% FBS and cytokines of interest onto 96-well dishes pretreated with a 0.1% gelatin solution.

Endothelial Cell Survival Assays

HUVECs between passages 6 and 8 were seeded onto 96-well dishes pretreated with a 0.1% gelatin solution. The cells were grown in EBM-2 solution supplemented with 2% FBS and cytokines of interest, then incubated for 3 days. On day 4, cells were incubated with Alamar Blue for 8h.

Fluorescence was measured at 530 nm excitation wavelength and 590 nm emission wavelength.

MVECs between passages 6 and 8 were seeded onto 96-well dishes pretreated with a 0.1% gelatin solution. The cells were grown in EBM-2 solution supplemented with 2% FBS and cytokines of interest, then incubated for 3 days. After 3 days, the media was refreshed by adding 100 µL EBM-2 solution supplemented with 2% FBS and cytokines of interest, and incubated for 3 additional days. On day 7, cells were incubated with Alamar Blue for 8h. Fluorescence was measured at 530 nm excitation wavelength and 590 nm emission wavelength.

<u>Tumor Cell IL-22 Proliferation Assays</u>

$1x10^3$ GL261 or $2.5x10^3$ EL4 cells were seeded onto 96-well dishes containing DMEM supplemented with 0,1, or 2% FBS, 1% antimycobacteria/antibacterial solution, and cytokines of interest. After 6 days, cells were incubated with Alamar Blue for 8h. Fluorescence was measured at 530 nm excitation wavelength and 590 nm emission wavelength.

Tumor Cell Antibody Treatment Assays

$1x10^3$ GL261 or $2.5x10^3$ EL4 cells were seeded onto 96-well dishes containing DMEM supplemented with 10% FBS, 1% antimycobacteria/antibacterial solution, and antibodies of interest. After 6 days, cells were incubated with Alamar Blue for 8h. Fluorescence was measured at 530 nm excitation wavelength and 590 nm emission wavelength.

Migration Assay

HUVECs (passage 6-8) were cultured and serum-starved as described in “Western blots.” The cells (10000 cells) in 150 µl of EBM-2 medium were then added to the upper chamber of 24 well 8 µm pore size cell culture inserts (Falcon) coated with 0.1% gelatin. The lower compartment was filled with 600 µL EBM-2 medium containing 1 µL/mL PBS with 0.1% BSA, 10 ng/mL IL-22, 25 ng/mL IL-22, 50 ng/mL IL-22, 100 ng/mL IL-22, or 50 ng/ml $VEGF_{165}$. The plates were incubated at 37°C to allow migration. After 4h, cells were fixed with 4% PFA for 30 min and then stained with crystal violet for 30 min at RT. Migrated cells on the bottom side of the insert membrane were quantified by counting whole area of the insert at 20X magnification. The experiments were carried out in quadruplicate and repeated two times. For MVEC, the migration assays were carried out as described for HUVECs, with the only alteration being an 8h incubation time.

EL4 in-vivo studies

Mice were injected subcutaneously with 1 x 10^6 cells in a 1:1 mixture of reduced growth factor basement membrane extract and sterile PBS. 5 days post injection, mice were sorted into groups based on weight and tumor size. They were given antibody treatment by intraperitoneal injection. Mice were again treated and tumor size measured every other day until conclusion of the study.

GL261 in-vivo studies

Mice were injected subcutaneously with 1 x 10^6 cells in a 1:1 mixture of reduced growth factor basement membrane extract and sterile PBS.

For C57BL/6 mice, 13 days post injection they were sorted into groups based on weight and tumor size. On day 16, tumor size was measured and mice were given antibody treatment by intraperitoneal injection. Mice were again treated and tumor size measured every other day until conclusion of the study.

For athymic nude mice: 5 days post injection they were sorted into groups based on weight and tumor size. They were given antibody treatment by intraperitoneal injection. Mice were again treated and tumor size measured every other day until conclusion of the study.

Quantification and Statistical Analysis

All image analysis was done using ImageJ. Cell counting was done manually using the cell counter function.

Statistical parameters, including the value of n, are indicated in the figure legends. All statistical analysis was conducted in Graphpad Prism software. One-way ANOVA, Two-way ANOVA, and Unpaired t-test with Welch's correction were used as statistical tests. All statistical tests use post-hoc analysis when appropriate to account for multiple comparisons. Test details are included in figure legends. Data are considered significant when $p < 0.05$. Significant p values are represented in the figures as follows: ***$p < 0.001$, **$p < 0.01$, *$p < 0.05$.

References

1. Folkman, J. & Klagsbrun, M. Angiogenic Factors. *Science (80-.).* **235,** 442–447 (1987).

2. Greenblatt, M. & Philippe, S. K. Tumor angiogenesis: Transfilter diffusion studies in the hamster by the transparent chamber technique. *J. Natl. Cancer Inst.* **41,** 111–124 (1968).

3. Folkman, J., Merler, E., Abernathy, C. & Williams, G. Isolation of a tumor factor responsible for angiogenesis. *J. Exp. Med.* **133,** 275–288 (1971).

4. Judah, F. Tumor angiogenesis: a possible control point in tumor growth. *Ann. Intern. Med.* **82,** 96–100 (1975).

5. Folkman, J. Tumor angiogenesis. *Adv. Cancer Res.* **19,** 331–358 (1974).

6. Senger, D. *et al.* Tumor Cells Secrete a Vascular Permeability Factor that Promotes Accumulation of Ascites Fluid. *Science (80-.).* **219,** 983–985 (1983).

7. Ferrara, N. VEGF and the quest for tumour angiogenesis factors. *Nat. Rev. Cancer* **2,** 795–803 (2002).

8. Leung, D. W., Cachianes, G., Kuang, W. J., Goeddel, D. V & Ferrara, N. Vascular endothelial growth factor is a secreted angiogenic mitogen. *Science* **246,** 1306–9 (1989).

9. Ferrara, N. Vascular endothelial growth factor: basic science and clinical progress. *Endocr. Rev.* **25,** 581–611 (2004).

10. Ausprunk, D. H. & Folkman, J. Migration and proliferation of endothelial cells in preformed and newly formed blood vessels during tumor angiogenesis. *Microvasc. Res.* **14,** 53–65 (1977).

11. Gross, J. L., Moscatelli, D. & Rifkin, D. B. Increased capillary endothelial cell protease activity in response to angiogenic stimuli in vitro. *Proc. Natl. Acad. Sci. U. S. A.* **80,** 2623–2627 (1983).

12. Klagsbrun, M. & D'Amore, P. Regulators of angiogenesis. *Annu. Rev. Physiol* **53,** 217–39 (1991).

13. Folkman, J. Angiogenesis in cancer, vascular, rheumatoid and other disease. *Nat. Med.* **1,** 27–31 (1995).

14. Ferrara, N., Gerber, H.-P. & LeCouter, J. The biology of VEGF and its receptors. *Nat. Med.* **9,** 669–76 (2003).

15. Karkkainen, M. J., Mäkinen, T. & Alitalo, K. Lymphatic endothelium : a new frontier of metastasis research. *Nat. Cell Biol.* **4,** 2–5 (2002).

16. Ferrara, N. & Davis-Smyth, T. The biology of vascular endothelial growth factor. *Endocr Rev* **18(1),** 4–25 (1997).

17. Ferrara, N. & Kerbel, R. S. Angiogenesis as a therapeutic target. *Nature* **438,** 967–74 (2005).

18. Gerber, H. *et al.* Vascular Endothelial Growth Factor Regulates Endothelial Cell Survival through the Phosphatidylinositol 3 ′ -Kinase / Akt Signal Transduction Pathway. *J. Biol. Chem.* **273,** 30336–30343 (1998).

19. Shweiki, D., Itin, A., Soffer, D. & Keshet, E. vascular endothelial growth factor induced by hypoxia may mediate hypoxia-induced angiogenesis. *Nature* **359,** 843–45 (1992).

20. Goldberg, M. & Schneider, J. Similarities between the Oxygen-sensing Mechanisms Regulating the Expression of Vascular Endothelial Growth Factor and Erythropoietin *. *J. Biol. Chem.* **269,** 4355–4359 (1994).

21. Liu, Y., Cox, S., Toshisuke, M. & Kourembanas, S. Hypoxia Regulates Vascular Endothelial Growth Factor Gene Expression in Endothelial Cells. *Circ. Res.* **77,** 638–643 (1995).

22. Tang, T. T. & Lasky, L. A. The Forkhead Transcription Factor FOXO4 Induces the Down-regulation of Hypoxia-inducible Factor 1 ⎵ by a von Hippel-Lindau Protein-independent Mechanism *. *J. Biol. Chem.* **278,** 30125–30135 (2003).

23. Neufeld, G., Cohen, T., Gengrinovitch, S. & Poltorak, Z. Vascular endothelial growth factor (VEGF) and its receptors. *Faseb J.* **13,** 9–22 (1999).

24. Iii, J. a S. *et al.* Regulation of angiogenesis by a non-canonical Wnt-Flt1 pathway in myeloid cells. *Nature* **474,** 511–515 (2011).

25. Liang, W. & Ferrara, N. The Complex Role of Neutrophils in Tumor Angiogenesis and Metastasis. *Cancer Immunol. Res.* **4,** 83–91 (2016).

26. Chen, W.-C. *et al.* Interleukin-17-producing cell infiltration in the breast cancer tumour microenvironment is a poor prognostic factor. *Histopathology* **63,** 225–33 (2013).

27. Coussens, L. & Werb, Z. Inflammation and cancer. *Nature* **420,** 860–867 (2002).

28. Murdoch, C., Giannoudis, A. & Lewis, C. E. Mechanisms regulating the recruitment of macrophages into hypoxic areas of tumors and other ischemic tissues. *Blood* **104,** 2224–34 (2004).

29. Siveen, K. S. & Kuttan, G. Role of macrophages in tumour progression. *Immunol. Lett.* **123,** 97–102 (2009).

30. Hanahan, D. & Coussens, L. M. Accessories to the crime: functions of cells recruited to the tumor microenvironment. *Cancer Cell* **21,** 309–22 (2012).

31. Iida, N. *et al.* Commensal Bacteria Control Cancer Response to Therapy by Modulating the Tumor Microenvironment. *Science (80-.).* **342,** 967–970 (2013).

32. Su, X. *et al.* Tumor microenvironments direct the recruitment and expansion of human Th17 cells. *J. Immunol.* **184,** 1630–41 (2010).

33. Maniati, E., Soper, R. & Hagemann, T. Up for Mischief? IL-17/Th17 in the tumour microenvironment. *Oncogene* **29,** 5653–62 (2010).

34. Numasaki, M. *et al.* IL-17 enhances the net angiogenic activity and in vivo growth of human non-small cell lung cancer in SCID mice through promoting CXCR-2-dependent angiogenesis. *J. Immunol.* **175,** 6177–89 (2005).

35. Chung, A. S. *et al.* An interleukin-17-mediated paracrine network promotes tumor resistance to anti-angiogenic therapy. *Nat. Med.* **19,** 1114–23 (2013).

36. Fridman, W. H., Pagès, F., Sautès-Fridman, C. & Galon, J. The immune contexture in human tumours: impact on clinical outcome. *Nat. Rev. Cancer* **12,** 298–306 (2012).

37. Curd, L. M., Favors, S. E. & Gregg, R. K. Pro-tumour activity of interleukin-22 in HPAFII human pancreatic cancer cells. *Clin. Exp. Immunol.* **168,** 192–9 (2012).

38. Miyagaki, T. *et al.* IL-22, but not IL-17, dominant environment in cutaneous T-cell lymphoma. *Clin. Cancer Res.* **17,** 7529–38 (2011).

39. Tartour, E. *et al.* Interleukin 17, a T-cell-derived cytokine, promotes tumorigenicity of human cervical tumors in nude mice. *Cancer Res.* **59,** 3698–704 (1999).

40. Yang, L. *et al.* Expression of Th17 cells in breast cancer tissue and its association with clinical parameters. *Cell Biochem. Biophys.* **62,** 153–9 (2012).

41. Xie, M. H. *et al.* Interleukin (IL)-22, a novel human cytokine that signals through the interferon receptor-related proteins CRF2-4 and IL-22R. *J. Biol. Chem.* **275,** 31335–9 (2000).

42. Dumoutier, L., Van Roost, E., Colau, D. & Renauld, J. C. Human interleukin-10-related T cell-derived inducible factor: molecular cloning and functional characterization as an hepatocyte-stimulating factor. *Proc. Natl. Acad. Sci. U. S. A.* **97,** 10144–9 (2000).

43. Dumoutier, L., Louahed, J. & Renauld, J.-C. Cloning and Characterization of IL-10-Related T Cell-Derived Inducible Factor (IL-TIF), a Novel Cytokine Structurally Related to IL-10 and Inducible by IL-9. *J. Immunol.* **164,** 1814–1819 (2000).

44. Dumoutier, L., Van Roost, E., Ameye, G., Michaux, L. & Renauld, J. C. IL-TIF/IL-22: genomic organization and mapping of the human and mouse genes. *Genes Immun.* **1,** 488–94 (2000).

45. Wolk, K. *et al.* IL-22 increases the innate immunity of tissues. *Immunity* **21,** 241–54 (2004).

46. Kotenko, S. V *et al.* Identification of the functional interleukin-22 (IL-22) receptor complex: the IL-10R2 chain (IL-10Rbeta) is a common chain of both the IL-10 and IL-22 (IL-10-related T cell-derived inducible factor, IL-TIF) receptor complexes. *J. Biol. Chem.* **276,** 2725–32 (2001).

47. Dumoutier, L., de Meester, C., Tavernier, J. & Renauld, J. C. New activation modus of STAT3. A tyosine-less region of the interleukin-22 receptor recruits stat3 by interacting with its coiled-coil domain. *J. Biol.*

Chem. **284,** 26377–26384 (2009).

48. Songyang, Z. *et al.* Specific motifs recognized by the SH2 domains of Csk, 3BP2, fps/fes, GRB-2, HCP, SHC, Syk, and Vav. *Mol. Cell. Biol.* **14,** 2777–2785 (1994).

49. Wolk, K., Kunz, S., Asadullah, K. & Sabat, R. Cutting edge: immune cells as sources and targets of the IL-10 family members? *J. Immunol.* **168,** 5397–402 (2002).

50. Sabat, R., Ouyang, W. & Wolk, K. Therapeutic opportunities of the IL-22-IL-22R1 system. *Nat. Rev. Drug Discov.* **13,** 21–38 (2014).

51. Dige, A. *et al.* Increased levels of circulating Th17 cells in quiescent versus active Crohn's disease. *J. Crohn's Colitis* **7,** 248–255 (2013).

52. Duhen, T., Geiger, R., Jarrossay, D., Lanzavecchia, A. & Sallusto, F. Production of interleukin 22 but not interleukin 17 by a subset of human skin-homing memory T cells. *Nat. Immunol.* **10,** 857–863 (2009).

53. Trifari, S., Kaplan, C. D., Tran, E. H., Crellin, N. K. & Spits, H. Identification of a human helper T cell population that has abundant production of interleukin 22 and is distinct from TH-17, TH1 and TH2 cells. *Nat. Immunol.* **10,** 864–871 (2009).

54. Rutz, S. *et al.* Transcription factor c-Maf mediates the TGF-β-dependent suppression of IL-22 production in TH17 cells. *Nat. Immunol.* **12,** 1238–1245 (2011).

55. Zheng, Y. *et al.* Interleukin-22, a T(H)17 cytokine, mediates IL-23-induced dermal inflammation and acanthosis. *Nature* **445,** 648–51 (2007).

56. Rutz, S., Eidenschenk, C. & Ouyang, W. IL-22, not simply a Th17 cytokine. *Immunol. Rev.* **252,** 116–32 (2013).

57. Kebir, H. *et al.* Human TH17 lymphocytes promote blood-brain barrier disruption and central nervous system inflammation. *Nat. Med.* **13,** 1173–5 (2007).

58. Wu, Z. *et al.* Interleukin 22 attenuated angiotensin II induced acute lung injury through inhibiting the apoptosis of pulmonary microvascular endothelial cells. *Sci. Rep.* **7,** 2210 (2017).

59. He, X. *et al.* The Effects of IL-22 on the Inflammatory Mediator Production, Proliferation, and Barrier Function of HUVECs. *Inflammation* **39,** 1099–1107 (2016).

60. Hurwitz, H. *et al.* Bevacizumab plus irinotecan, fluorouracil, and leucovorin for metastatic colorectal cancer. *N. Engl. J. Med.* **350,** 2335–42 (2004).

61. Ferrara, N. Microvascular Density as a Predictive Biomarker for Bevacizumab Survival Benefit in Ovarian Cancer: Back to First Principles? *J. Natl. Cancer Inst.* **109,** 16–17 (2017).

62. Martin, L. K. *et al.* VEGF remains an interesting target in advanced pancreas cancer (APCA): results of a multi-institutional phase II study of bevacizumab, gemcitabine, and infusional 5-fluorouracil in patients with APCA. *Ann. Oncol.* **23,** 2812–20 (2012).

63. Crawford, Y. & Ferrara, N. VEGF inhibition: insights from preclinical and clinical studies. *Cell Tissue Res.* **335,** 261–9 (2009).

64. Dirkx, A. E. M. *et al.* Anti-angiogenesis therapy can overcome endothelial cell anergy and promote leukocyte-endothelium interactions and infiltration in tumors. *FASEB J.* **20,** 621–30 (2006).

65. Kirchberger, S. *et al.* Innate lymphoid cells sustain colon cancer through production of interleukin-22 in a mouse model. *J. Exp. Med.* **210,** 917–31 (2013).

66. Tepper, R. I., Pattengale, P. K. & Leder, P. Murine interleukin-4 displays potent anti-tumor activity in vivo. *Cell* **57,** 503–12 (1989).

67. Staton, C. a, Reed, M. W. R. & Brown, N. J. A critical analysis of current in vitro and in vivo angiogenesis assays. *Int. J. Exp. Pathol.* **90,** 195–221 (2009).

68. Xin, H., Zhong, C., Nudleman, E. & Ferrara, N. Evidence for Pro-angiogenic Functions of VEGF-Ax. *Cell* **167,** 275–284.e6 (2016).

69. Arnaoutova, I. & Kleinman, H. K. In vitro angiogenesis: endothelial cell tube formation on gelled basement membrane extract. *Nat. Protoc.* **5,** 628–35 (2010).

70. Besnard, A. G. *et al.* Dual role of IL-22 in allergic airway inflammation and its cross-talk with IL-17A. *Am. J. Respir. Crit. Care Med.* **183,** 1153–

1163 (2011).

71. Ferrara, N., Houck, K., Jakeman, L. & Leung, D. W. Molecular and biological properties of the vascular endothelial growth factor family of proteins. *Endocr Rev* **13,** 18–32 (1992).

72. OShea, J. J., Gadina, M. & Schreiber, R. D. Cytokine signaling in 2002: New surprises in the Jak/Stat pathway. *Cell* **109,** 121–131 (2002).

73. Lejeune, D. *et al.* Interleukin-22 (IL-22) activates the JAK/STAT, ERK, JNK, and p38 MAP kinase pathways in a rat hepatoma cell line. Pathways that are shared with and distinct from IL-10. *J. Biol. Chem.* **277,** 33676–82 (2002).

74. Robertson, S. C., Tynan, J. A. & Donoghue, D. J. RTK mutations and human syndromes - When good receptors turn bad. *Trends Genet.* **16,** 265–271 (2000).

75. Gschwind, A., Fischer, O. M. & Ullrich, A. The discovery of receptor tyrosine kinases: targets for cancer therapy. *Nat. Rev. Cancer* **4,** 361–370 (2004).

76. Andoh, A. *et al.* Interleukin-22, a member of the IL-10 subfamily, induces inflammatory responses in colonic subepithelial myofibroblasts. *Gastroenterology* **129,** 969–984 (2005).

77. Bezbradica, J. S. & Medzhitov, R. Integration of cytokine and heterologous receptor signaling pathways. *Nat. Immunol.* **10,** 333–339 (2009).

78. Yamauchi, T. *et al.* Tyrosine phosphorylation of the EGF receptor by the kinase Jak2 is induced by growth hormone. *Nature* **390,** 91–96 (1997).

79. Tan, A. H.-M. & Lam, K.-P. Pharmacologic inhibition of MEK-ERK signaling enhances Th17 differentiation. *J. Immunol.* **184,** 1849–57 (2010).

80. Nardinocchi, L. & Sonego, G. Interleukin-17 and Interleukin-22 promote tumor progression in human non-melanoma skin cancer. *Eur. J. …* 1–28 (2014). doi:10.1002/eji.201445052.This

81. Gerber, H.-P. *et al.* Mice expressing a humanized form of VEGF-A may provide insights into the safety and efficacy of anti-VEGF antibodies. *Proc. Natl. Acad. Sci. U. S. A.* **104,** 3478–83 (2007).

82. Liu, X., Yang, J. & Deng, W. The inflammatory cytokine IL-22 promotes murine gliomas via proliferation. *Exp. Ther. Med.* **13,** 1087–1092 (2017).

83. Folkman, J. Is angiogenesis an organizing principle in biology and medicine? *J. Pediatr. Surg.* **42,** 1–11 (2007).

84. Jain, R. K. Normalizing tumor vasculature with anti-angiogenic therapy: a new paradigm for combination therapy. *Nat. Med.* **7,** 987–989 (2001).

85. Kerbel, R. & Folkman, J. Clinical translation of angiogenesis inhibitors. *Nat Rev Cancer* **2,** 727–739 (2002).

86. Lichtenberger, B. M. *et al.* Autocrine VEGF signaling synergizes with EGFR in tumor cells to promote epithelial cancer development. *Cell* **140,** 268–79 (2010).

87. Liang, W.-C. *et al.* Cross-species vascular endothelial growth factor (VEGF)-blocking antibodies completely inhibit the growth of human tumor xenografts and measure the contribution of stromal VEGF. *J. Biol. Chem.* **281,** 951–61 (2006).